Indirect methods to determine the fundamental parameters of a stellar-mass black hole and the discrepancies found in the measurement

Report

by team

Annihilators

Under the guidance of **Mr. Sundar M N**

Department of Astrophysics

Society for Space Education Research and Development

Bangalore

December, 2021

Society for Space Education Research & Development

EDUCATE - INSPIRE - INNOVATE

Team Members

1. Sneha Singh - Team Leader
   5^{th} Year, Integrated M.Sc Physics,
   Birla Instutute of Technology, Mesra

2. Jatin Chopra - Team Co-Leader
   3^{rd} Year, B.Sc Physics,
   Savitribai Phule Pune University (Nowrosjee Wadia College), Pune

3. Piyush R Gone - Team Coordinator
   1^{st} Year, M.Sc Physics,
   St. Joseph's College, Bangalore

4. Gagan A V
   3^{rd} Year, BSc PCM,
   Christ (Deemed to be University), Bengaluru

5. Neel Nilesh Panchal
   3^{rd} Year, BTech Electronics Engineering,
   SVKM's Dwarkadas Jivanlal Sanghvi College of Engineering, Mumbai

6. Pathipati Sahithi Chowdary
   3^{rd} Year, BTech Mechanical Engineering,
   Sastra Deemed University, Thanjavur

7. Sreeporna, 2^{nd} Year, MSc in Physics,
   Cotton University, Guwahati

8. Uttam Kumar
   2^{nd} Year, BTech Engineering Physics,
   NIT Hamirpur, Patna

9. Pragyan Jyoti Dutta
   2^{nd} Year, Integrated MSc. in Physics ,
   Tezpur University, Tezpur

Acknowledgments

Firstly, we would like to express our gratitude towards Society for Space Education, Research and Development (SSERD) for providing us an opportunity of being an Intern. Through this Internship program, we were able to work under the guidance of a supervisor and co-supervisor, where we learned new and helpful things. We would also like to extend our special thanks to the society and the people for organizing this Internship program.
Secondly, we would like to express our special thanks of gratitude and give great recognition to our supervisor Mr. Sundar M N, who gave us the golden opportunity to do this wonderful project on the topic *"Indirect methods to determine the fundamental parameters of a stellar-mass black hole and the discrepancies found in the measurement"*, which also helped us in doing a lot of research. Along with that, we are grateful to co-supervisor Prateek Boga, who helped us throughout our internship with the technical and literature queries and kept us motivated.
Lastly, we would like to say that this Internship has been beneficial to every member of our team and it has been an amazing experience.

Abstract

Looking at the fundamental parameters of a stellar mass BH and indirect methods to determine them,

Keywords:

Stellar mass black hole, Fundamental Parameters, Mass, Spin, Mass Function, X-ray transients, QPOs.

Contents

List of Figures

List of Tables

List of Symbols

1 Introduction

1.1 What is a Black Hole?

A Black Hole (BH) is a region in space-time where the gravitational pull is so much that even light cannot get out. A BH is not visible as gravity pulls all the light in the middle of the black hole. A BH is formed when the mass of the gravitating object of mass M becomes smaller than its gravitational radius.

$$r_s = \frac{2GM}{c^2} \tag{1.1}$$

where, M is the mass of the non spinning BH, c is speed of light, and G is the Universal Gravitational constant.

The boundary surface that restricts the no-return region is called the event horizon. Black holes are different from all astronomical objects. We cannot see BHs, but we can see how intense gravity can affect the star and gas around the BH and through gravitational waves. When a black hole and a star are close together, high-energy light is made. This kind of light cannot be seen with human eyes. Scientists use satellites and telescopes in space to see high-energy light. The high resolution of the Hubble Space Telescope made it possible to see the effects of the gravitational attraction of some of these objects on their surroundings. Hubble has also proved that supermassive black holes are most likely present at the centers of most, if not all, large galaxies.

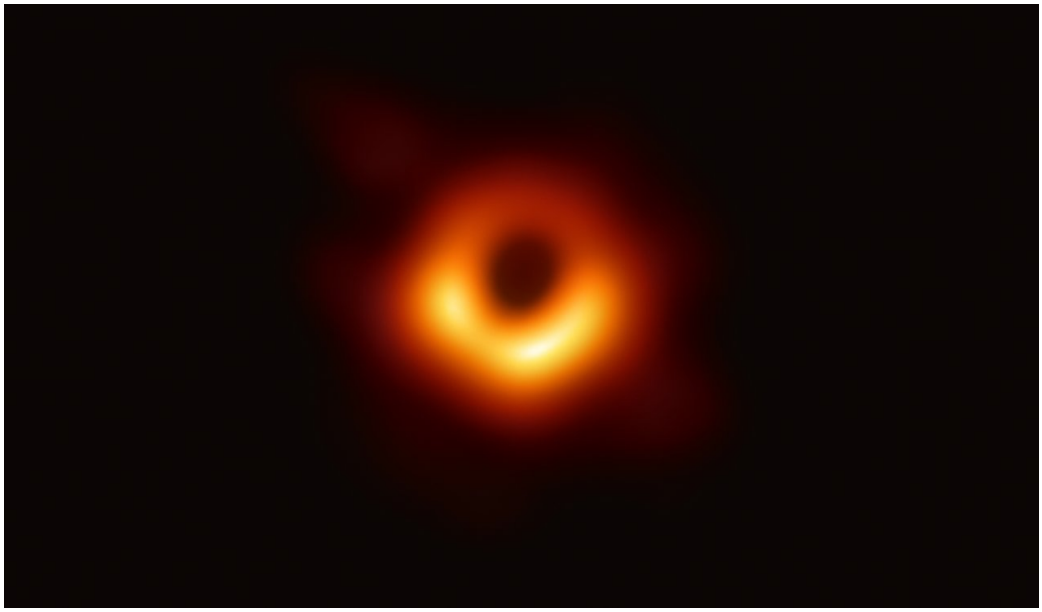

Figure 1.1: First Image of a Black Hole - M87 by the Event Horizon Telescope (EHT) collaboration et al.

The properties of a black hole are so unusual that even Albert Einstein could not accept that these weird objects exist in reality despite being the solutions of the relativity theory. According to general relativity, gravity is the curvature of space-time. So, considering this, a BH is 'plenty of nothing,' just self-supported empty curved space-time. [16]

Black holes are a striking example of a prediction of Einstein's theory of gravity, general relativity. Although it took many decades before the physical concept of a black hole was fully understood and widely accepted, recent years have seen rapid advances on both the observational and theoretical side, which we want to illustrate in this brief note with three examples. Black holes have become an astrophysical reality.

1.2 Classification of BHs

Based on mass, BHs can are classified into these types:

1. Micro Black holes.
   Also known as quantum mechanical blackholes or mini blackholes, for which quantum effects play an important role. These blackholes are theorized to be as small as an atom, but with a mass rivaling that of a large mountain. None of these micro black holes have been observed yet, however, so their existence remains purely theoretical.

2. Primordial Black Holes.
   The mass of Primordial black holes (PBHs) is comparable to or less than Earth's. These purely hypothetical objects could have been formed through the gravitational collapse of regions of high density at the time of the Big Bang. PBHs was born when

the universe was still young, within a mere second of the Big Bang. Furthermore, depending on just how soon after the Big Bang these first black holes formed, they could range from about 0.00001 times the mass of a paperclip to about 100,000 times the mass of the Sun.

3. Stellar Mass Black Holes
   The masses of Stellar-mass black holes are in the range of about 4 and 100 solar masses and result from the core-collapse of a massive star at the end of its life.

4. Intermediate Mass Black Holes
   Intermediate-mass black holes fall between stellar-mass black holes and super-massive black holes. BH of this type is neither too big nor too small and is rare. Such a BH is thought to form when multiple stellar-mass black holes undergo a series of mergers with one another. There are theories for how intermediate BHs may have formed.
   a. Due to merging of stellar mass BHs and other compact objects by means of accretion.
   b. They may form in a runaway collision of massive stars in dense stellar clusters.
   c. They might also be primordial BHs formed in the early universe, similar to micro BHs.

5. Supermassive Black Holes
   Supermassive black holes weigh between 10^5 and 10^{10} solar masses and are found at the centers of the giant galaxies. Black holes tend to grow larger and larger through mergers, which is an expected case for supermassive black holes. Although there are many theories about how this type of black hole forms, the most compelling is that they grow larger through a runaway chain reaction of colliding stars and black holes. In such a scenario, the seed of the supermassive black hole continuously merges and gobbles up more and more material, eventually getting so massive that it "sinks" toward the center of its galaxy.

Instead of these there are also other types of BHs that come up when quantum mechanics applied to understand gravity or when cosmologists explore the early universe

1. Plank mass: These have a mass of 10^{-7} Kgs and size is about 100 billion billion times smaller than a photon.

2. Primordial: These BHs can have a mass greater than 10 trillion Kgs and would have formed soon after the Big-bang and still exist today.

Based on rotation and charge, BHs can be classified into four types which are as follows:

1. Schwarzschild Black Hole
   They are also known as a 'static black hole,' which does not rotate and has no electric

charge. It is characterized solely by its mass.

no angular momentum	$R_g = 2M$
no charge	$M^2 = M_{ir}^2$
no energy extraction	$A = 4\pi R_g^2 = 16\pi M^2$

Table 1.1: Schwarzschild Black Hole: Physical and Mathematical Description

2. Kerr Black Hole
   They have no electric charge, but the reduction of angular momentum can extract energy.these rotate and are flattened at the poles, and can only be described by their mass and spin(angular momentum)

no charge	$r_+ = 2M + \sqrt{M^2 - a^2}$
energy extraction can be done by reduction of angular momentum	$M^2 = M_{ir}^2 + L^2/4M_{ir}^2$
	$A = 4\pi(r_+^2 + a^2)$

Table 1.2: Kerr Black Hole: Physical and Mathematical Description

3. Reissner-Nordström Black Hole
   They have no angular momentum but are electrically charged, and hence energy can be extracted by the reduction of the net charge.

no angular momentum	$r_+ = M + \sqrt{M^2 - Q^2}$
charged	
energy extraction by reduction of net charge	$M^2 = M_{ir} + (Q^2/4M_{ir})^2$
	$A = 4\pi(r_+^2)$

Table 1.3: Ressiner-Nordström Black Hole: Physical and Mathematical Description

4. Kerr –Newman Black Hole
   They have both angular momentum and electric charge and thus energy can be extracted by both mass and spin.

1.3 Stellar Mass BH

Stellar-mass black holes are the final stage of the evolution of a massive star. It forms when a massive star reaches the end of its life and implodes, collapsing in on itself. If the

imploding star is between eight and 20 times the mass of the Sun, however, it will not form a black hole. Instead, the collapsing material will rebound off its core, causing it to erupt as a supernova. According to the Chandrasekhar limit, the upper limit of the white dwarf mass is about 1.4 $M_{\odot}$. The critical mass is about 3 $M_{\odot}$, or a bit less for neutron stars. If, after the collapse of a massive progenitor star, the mass of the central collapsing core is more significant than these limits, one expects a black hole formation.

But if the collapsing star is more significant than about 20 times the mass of the Sun, its core isn't strong enough to stop the implosion. No mechanism can prevent such a star from collapsing into a black hole.

Depending on the initial size of the imploding star, the resulting stellar-mass black hole can reach up to about 100 or more times the mass of the Sun.

Using the information concerning the motion of the star companion, the mass function can be found for the binary and can be used to estimate the mass of the black hole. When its mass is larger than 3 $M_{\odot}$, one concludes that the star's companion in the binary is a candidate for a black hole.

Cygnus X-1 is the first discovered black hole binary candidate, followed by LMC X-3.

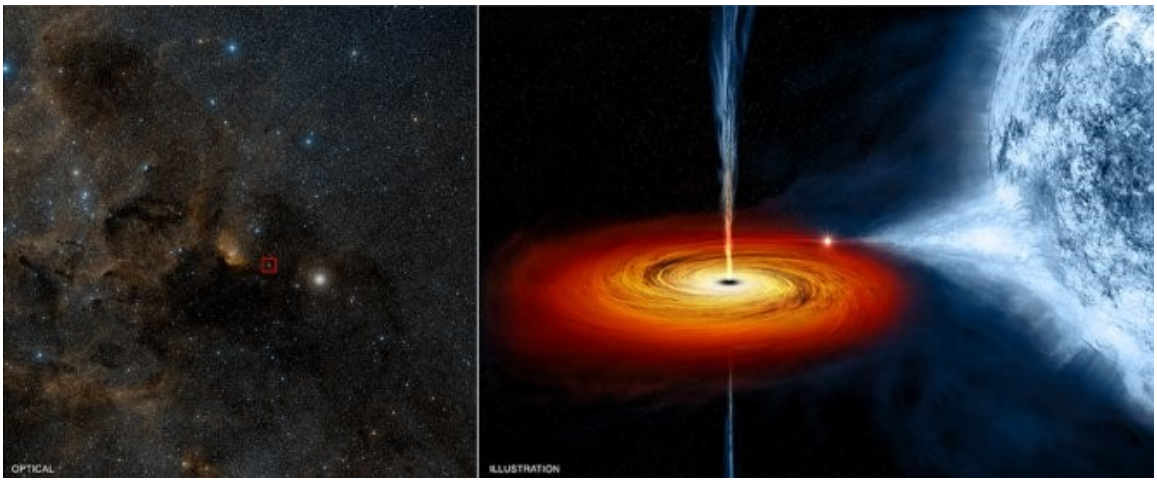

Figure 1.2: Cygnus X-1: A Stellar Mass Black Hole

2

Fundamental Parameters of a Black hole

When a star becomes a black hole, all of its familiar characteristics including color, temperature, luminosity no longer exist. The three fundamental parameters that exist are mass, spin/angular momentum and charge. Here these fundamental parameters have be discussed in detail.

2.1 Mass

Mass is one of the most important fundamental parameter of a black hole. Stellar mass black holes have a mass range of 3 - 20$M_{\odot}$. Over the years, various observations and surveys have found stellar-mass black holes in many binaries of our galaxy and other galaxies. Kalogera & Baym 1996 [24], showed that there couldn't be any neutron star more massive than 3$M_{\odot}$.

If the mass measurements of any potential stellar-mass black hole are higher than 3$M_{\odot}$ then we can classify the candidate as a stellar mass black hole. Such mass measurements and estimations are made using cautious radial velocity measurements of the binary partner.

The mass of the invisible object in the binary system is given by the mass function $f(M_X)$. The mass function gives the lower limit of the mass of the unseeable object. Mass function depends on the period of the orbit, Amplitude of radial velocity and eccentricity of the orbit. The mass function is given by the following equation, [49]

$$f(M_X) = \frac{1}{2\pi G} P_{orb} K_{opt}^3 (1 - e^2)^{\frac{3}{2}} \tag{2.1}$$

It is clearly evident from the above equation that the mass of the black hole can be subjected to errors produced while measuring the orientation of the orbit, and the nature of the binary companion. At present, there are precise mass measurements of ~ 20 stellar mass black hole. For more information please refer to Chapter 3.1

2.2 Spin

Mass and spin are more original properties of every elementary particle. We know that in general relativity, matter is represented by the energy-momentum tensor which provides a description of the mass density distribution in space-time so that the mass-energy concept is sufficient to define the properties of the classical, macroscopic bodies; but if we go down to a microscopic level, we find that matter is formed by elementary particles and are characterized not only by mass but also by a spin. [16]

In the above section '1.1', it is mentioned that the gravitational collapse of the spherical non-rotating black mass produces a spherically symmetric black hole when the radius of the collapsing body becomes less than the gravitational radius. The gravitational collapse of a massive spinning star or the collapse or collision of a collection of compact objects, stars, or gas with a total non-zero angular momentum is responsible for the formation of rotating black holes. All black holes are expected to be rotating black holes since all known stars rotate and realistic collisions have non-zero angular momentum.

For understanding such empirical issues as how gamma-ray bursts are powered and how black holes' launch jets and other outflows that inject energy into the surrounding medium and affect structure formation on the scale of galaxies and even clusters of galaxies, the knowledge of black hole spin is very important. One of the relation between spin and mass of the stellar mass black hole is,

$$a_* = \frac{cJ}{GM^2} \tag{2.2}$$

where, a_* = spin parameter, c = speed of light , J = Angular Momentum, M = Mass.

In a paper, through their work the authors have concluded that spinning black holes are more massive than non-spinning black holes for a given mass. However, slowly spinning black holes can turn out to be more massive than spinning black holes if mass at their formation stage was higher compared to faster spinning black holes. [38]

There are several methods through electromagnetic waves or gravitational waves from

which spin of a stellar mass black hole can be determined. Different methods such as fitting of continuum X-ray spectrum, Fe-line profile method etc. are discussed in the next chapter in detail.

Cygnus X-1, the first black hole, which was discovered in 1972. It is measured to 6 percent accuracy its distance (1.86 kpc) using the VLBA and its mass (14.8 solar masses) using extensive optical data. Chandra data reveal that the compact object is a near-extreme Kerr hole with a spin $a/M > 0.95$.

2.3 Charge

Charge is denote by Q, The Einstein field equations, which describe gravity in general relativity, have four known black hole solutions. Reissner–Nordström black holes (without spin) and Kerr–Newman black holes (with spin) are two of them that have charge. Charged black holes can be explained in theory, but its astrophysical conditions that result to their development may appear to be complex.

The formation of retro-lensing images also known as mirage due to the massive gravitational field effects near black holes can be used to find out the charge of the black hole. Measuring mirage shapes should can be useful to calculate the black hole mass and inclination angle. In the extreme charge situation of a Reissner-Nordström black hole, the charge changes the size of the shadows by up to 30%. If the other black hole parameters are known with sufficient precision, the charge of the black hole can be calculated by measuring the shadow size. In general, a measurement of the mirage shape (in size) permits all of the black hole parameters (mass, spin, charge) to be evaluated. [51]

3

Indirect methods to determine the various fundamental parameters

Since not even light can pass through a BH there is no direct method to determine the fundamental parameters of a BH. We can detect them by the energy emitted from accretion disks formed as material falls towards them or based on their gravitational influences on other objects that we can observe. Thus, there are various

3.1 Methods to determine Mass

Following are the various methods to determine mass and mass function of a stellar mass BH.

3.1.1 X-Ray Transients

Measurement of mass is very crucial in the study of Stellar mass black holes. Cowley 1992; in his work claimed that there must be about 1000-3000 Stellar Mass Black Holes in our galaxy. However, only about 20 stellar mass black holes have been observed yet. [10] Since black holes emit no electromagnetic energy or radiation, studying and detecting them is no easy task. Luckily, it's easy to detect and observe accreting compact binary systems. About 20 X-Ray binary systems which are X-Ray transients are found.[43][45]

As discussed in section 2.1, the mass function yields the smallest possible mass of the black hole in a binary system. Spectroscopic studies would provide the radial velocity curve of the binary partner star. The radial velocity curve provides the orbital period P_{orb} and the semi-amplitude radial velocity of the binary partner K_c. The mass function is given as follows,

$$f(M_x) = \frac{K_c^3 P_{orb}}{2\pi G} = \frac{M_x sin^3(i)}{(1+q)^2} \tag{3.1}$$

Thus, the mass function equation depends upon the mass ratio (q) and an orbital parameter called inclination angle (i). Hence, It's very crucial to measure these parameters accurately to minimize error and get the actual mass of the black hole.

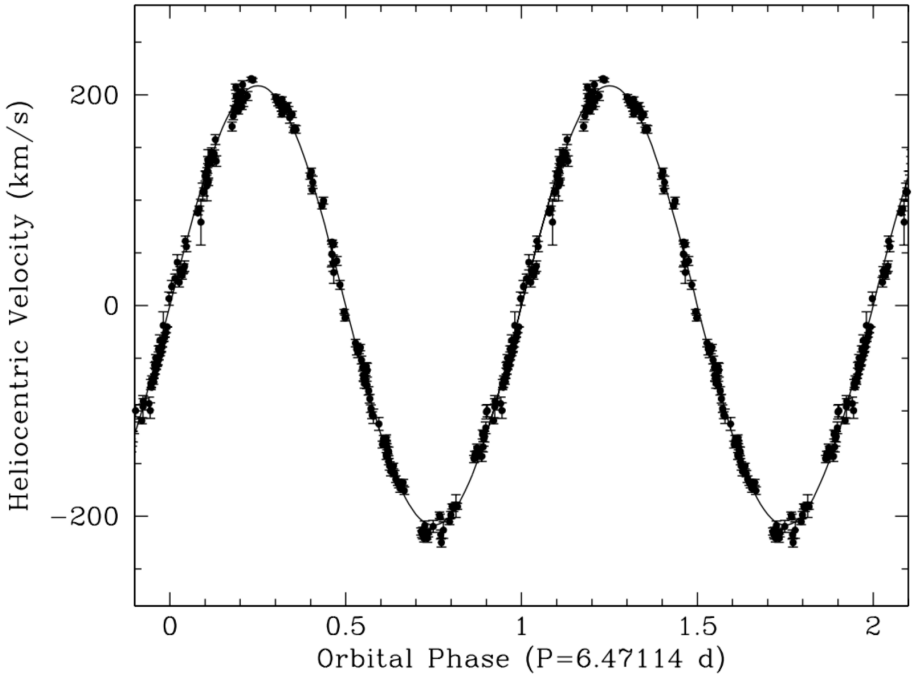

Figure 3.1: Radial velocity curve of the K0 donor star in the XRT V404 Cyg [8]

3.1.2 Measurement of Mass ratio (q)

Measurement of the rotational broadening ($Vsin(i)$) from photospheric lines of the binary partner is the ideal way to estimate the mass ratio (q). Making a simple approximation of sphericity, we can estimate q using this equation, [50]

$$Vsin(i) = 0.462 \times K_c q^{(\frac{1}{3})}(1+q)^{(\frac{2}{3})} \tag{3.2}$$

Where, K_c stands for the semi-amplitude radial velocity of the binary partner, q stands for mass ratio (M_{star}/M_{bh}) For accurate measurement of $Vsin(i)$, the observed spectra are compared and analysed to a slowly rotating template. The statistical errors in the calculation of $Vsin(i)$ are more significant than the systematical errors. Therefore, the mass ratios obtained are a good estimate of the system under study. [8]

3.1.3 Measurement of Inclination angle (i)

The binary system's inclination angle is determined via optical and near-infrared light curve fitting with ellipsoidal models. Due to the tidal distortion of the binary partner and the uneven surface brightness of the partner, a double-humped modulation is created in the light curves of the X-Ray transients. There is a potent relationship between the amplitude of double-humped modulation and the angle of inclination. Synthetic models use this relationship to calculate the inclination of the system. Kurucz and nextgen are synthetic models that provide the best solutions. [41] Various groups have worked and developed their synthetic models to measure the inclination angle. Surprisingly, the values calculated by them are in a narrow range of $64 - 71^{\circ}$. [41][40]

3.1.4 Errors

As discussed above, mass function depends on the angle of inclination (i) and the mass ratio (q). Thus, any error in their measurements will have a ripple effect in the determination of mass function. Refer to chapter 4 for few discrepancies and the mass function measurement. There are various values and discrepancies in the mass function measurements computed by various groups. It is believed that these discrepancies are the result of systematic errors due to adulteration from non-stellar light sources. There are two main systematic error sources which are,

1. Superhump Modulation
2. Aperiodic Variations

3.1.4.1 Superhump Modulations

Superhump Modulation is believed to be a distortion wave produced eccentric accretion disc which precesses on a timescale of a few percentages longer than the binary system's orbital period. [39] The fact that this modulation's period is slightly longer than the system's period rules out any geometric explanation for this phenomenon and is widely believed to be caused by intrinsic luminosity variations. Superhump waves distort the ellipsoidal light curve of the system under observation and study. See below for example, Fig.3.2

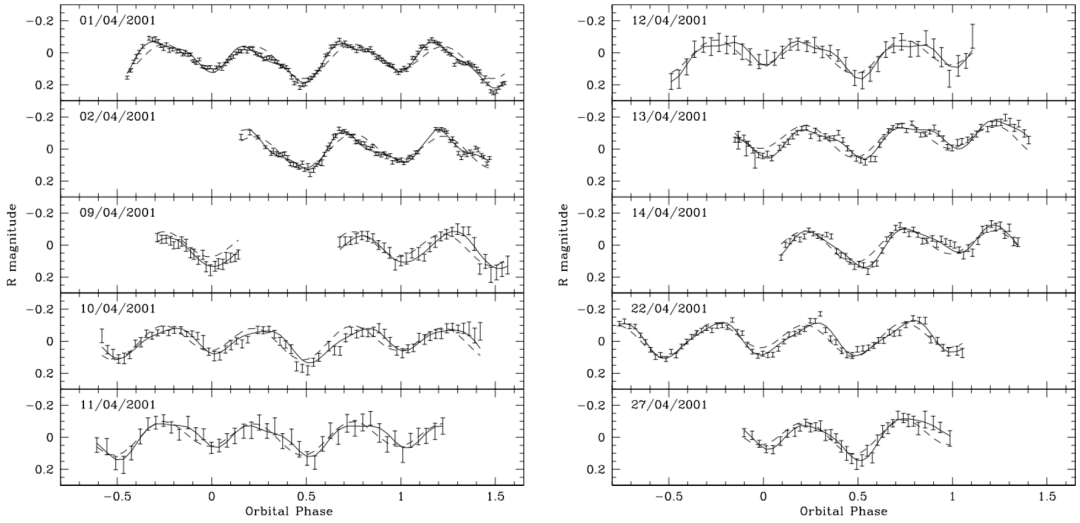

Figure 3.2: Ellipsoidal light curves distorted by a superhump in XTE J1118+480. A combined model of an ellipsoidal plus superhump waves (continuous line) provides a better description of the data than a pure ellipsoidal fit (dashed line). From Zurita et al. (2002).

There are changes and variations in the shape of the light curve and the relative heights between the maximum and the minimum. Without considering this error source the measurement of mass would not be accurate. Therefore it's very crucial to remove these superhump waves to get the actual light curve.

3.1.4.2 Aperiodic Variations

Aperiodic and random variations are another potential source of error in the mass measurement process. Optical flares due to the binary companion can be potent sources of errors. Work done by various groups has shown that all quiescent XRT change their brightness from 0.06 mag to 0.6 mag. [52][23] Moreover, these variations are very potent in cooler binary partners. It is believed that these variations have magnetic origins, synchrotron emission from disc jets. Sadly, the true origins of these variabilities are still unknown.
Cantrell et al(2008)[6] found two states of variabilities for system A0620-00 using multicolour quiescent photometry. In their work, they noticed that the system A0620-00 show mainly two prime states of variations. They named them as active state and the passive state. In the colour-magnitude diagram, the systems can be identified to be in different regions. In the passive state, the system becomes redder and displays very little flaring than in the active state. This can be very well displayed in the Fig.3.6.

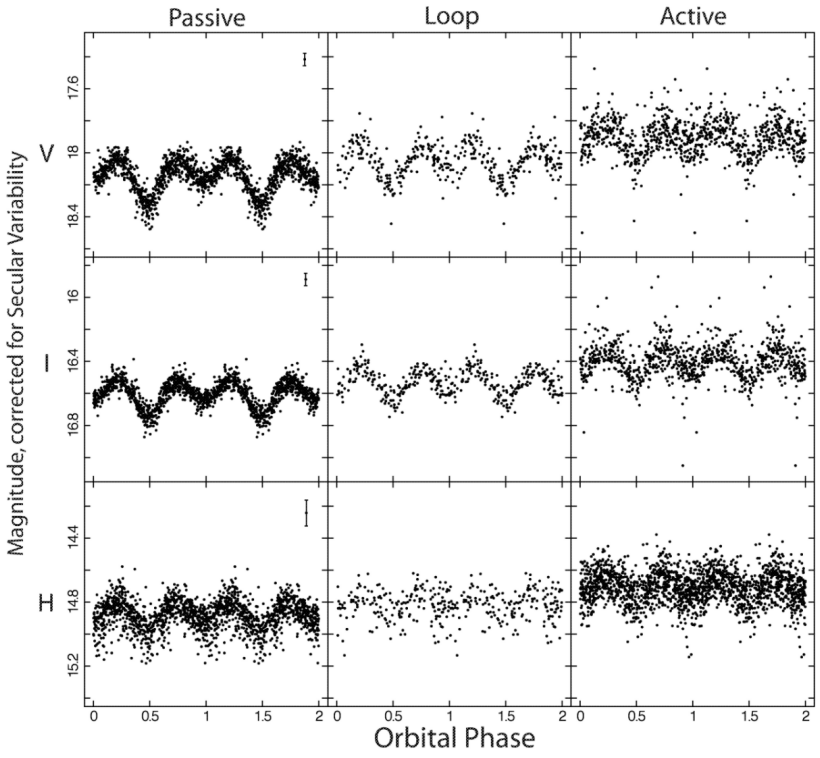

Figure 3.3: Ellipsoidal light curves of A0620-00 in three different quiescent states: passive (left panels), loop (middle panels) and active (right). The strength of the aperiodic variability increases from the passive to the active state. From Cantrell et al. (2008).

Cantrell et al (2010)[7] used this fact and obtained the angle of inclination of the system 10° higher than old measurements.

3.1.5 Mass Function from Gravitational Wave Measurements

Gravitational waves are produced by cataclysmic events, in our case colliding black holes i.e. Binary Black Holes (BBHs) and to detect these event Laser Interferometer Gravitational-wave Observatory (LIGO) and Virgo interferometer. The assumption made was all the BHs with mass less than $\sim 100\, M_\odot$ originate from the demise of massive stars (i.e. unless stated otherwise, we neglect previous mergers, primordial black holes, etc.). To this day, only 29 such BHs have been detected.

The stellar initial mass function (IMF) is well-described by a multi-part power-law $P(M) \propto M^{-\alpha}$,with α taken to be $2:3 \pm 0:7$ for $M > 1\, M_\odot$, and is only sensitive to slope in the higher mass range. Hence they considered massive BBHs, whose mass we denote by M_1, will also follow a powerlaw mass distribution $P_{BH}(M_1) \propto M_1^{\alpha}$, with the value of α corresponding to the relevant mass range for the progenitor stars. In this particular paper the author has assumed the value of $\alpha = 2.35$ for fiducial value [28]. After the first observations of the three coalescence events GW150914, LVT151012 and GW151226, LIGO has constrained α to be $2.5^{+1.5}_{-1.6}$ at 90% credible interval.

The lower bound and the upper bound is by various authors for stellar-mass BHs to be 2-5 $M_\odot$ and ($\simeq 150\, M_\odot$) and the theoretical distribution function is given by, [28] [43][14]

$$P(M_1) \propto M_1^{\alpha} H(M_1 - M_{gap}) e^{-M_1/M_{cap}} \tag{3.3}$$

Where, M_1 is the mass of the heavier binary component, α is a power law with a fiducial value of 2:35, M_{gap} is the NS-BH transition cutoff, which we take to be sharp, M_{cap} is a (shallower) exponential upper cutoff on the BH mass and H is the Heaviside function.

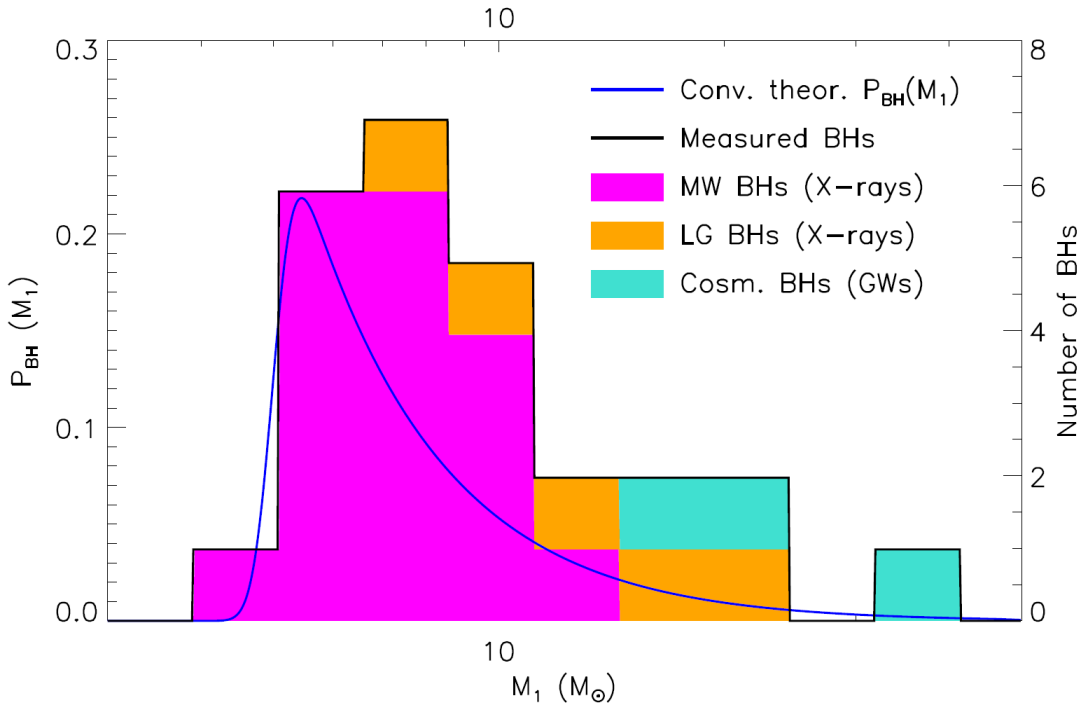

Figure 3.4: The distribution function $P_{BH}(M_1)$ of the heavier BH mass M1 in either BBHs or BH-star binaries. The blue line shows the theoretical prediction of Eq. (3.3) convolved with a Log Normal distribution that has a 5% error. The black histogram describes the observed distribution from 26 BHs. The red histogram is similar, but is based solely on the 18 dynamically confirmed BHs observed in X-rays that originate in the Milky Way. The yellow histogram stacked on the red one includes the five BHs observed through X-rays at LMC, IC 10, M33 and NGC 300. The green histogram stacked on the other two includes the three M1 masses detected by LIGO.

In Fig. 3.4, we plot the mass distribution of BHs observed in X-ray binaries as well as merging BBHs. For the latter we only show the mass of the heaviest of the two BHs M_1 (before the merger event). In solid blue we plot the theoretical probability density function of M_1, Eq. (3.3). To account for reasonable uncertainty in the mass estimation, the BHMF with a log-normal distribution with a 5% error in the mass.

While the statistics based on GW measurements in this figure are quite modest, it is expected up to thousands of BBHs to be observed in the next decade. These observations would surpass the X-ray sample in size by a significant factor and affect the observed mass distribution.

This is also dependents on the redshift distribution of the BH-BH merger, with gravitational waves we detect probe merger events of BH binaries at cosmological distances up to Gpcs, which is upto $z \sim 0.3$ in terms of redshift, In future with experiments like Einstein Telescope we might reach up to $z \sim > 10$.[46]

A simplified parametrization given by,

$$R(z) = R_a(1+z)^{R_b} \tag{3.4}$$

3.1.6 Comparison of BBH and BHXRBs

Stellar mass black holes are formed from the collapse of massive stars. Before the identification of gravitational waves, stellar mass black holes were observed using X-ray binaries. A lot of these black holes can be found in mass exchange binaries i.e., a star is close enough to a black hole such that the black hole starts accreting material from the companion star. During this process, the accreting material reaches very high temperatures that it glows brightly in X-rays, indirectly providing us a means to observe the motion of matter. In black hole X-ray binary system there are more binaries whose mass of companion star is low, only a few of them have companion stars which are massive. These binaries are observed during their episodic outbursts. X- ray binaries are classified into two types based on the companion star and the type of accretion.

- Low mass X-ray binaries (LMXRBs) and,
- High mass X-ray binaries (HMXRBs).

LMXRBs have low mass companion star and accretion powered by Roche lobe accretion whereas HMXRBs have high mass companion star and accretion is wind fed i.e., the compact object accretes from the wind of the star. The massive star produces powerful stellar winds and a part of the wind is captured by the gravitational filed of the black hole. LMXRBs, HMXRBs and BBHs all originate from massive stars but their evolutionary pathways can be different which give rise to astrophysical selection effects and thus require different detection criteria. In black hole X-ray binaries, the component black holes observed in gravitational wave binary black holes are generally more massive and rotate slowly compared to those observed in X-ray binaries. When comparing black hole masses between black hole X-ray binaries and binary black hole system we should not forget that gravitational wave method observations measure two mass distributions one is primary

mass i.e., mass of the more massive black hole and the other is secondary mass whereas BHXRBs have only one black hole. The masses of BHs in observed LMXBs are much smaller than the fundamental mass distribution of BBHs. This mismatch, however, could be attributed to a hidden variable: companion masses. The reported LMXB BH masses are consistent with the BBH primary mass distribution when accounting for binary component pairing and confining to BHs with low mass secondaries. The observed HMXB BH masses are consistent with the underlying BBH fundamental mass distribution.

3.2 Methods to determine Spin

Currently, there are three primary techniques that are delivering measurements of spin. They are:

1. Fitting the thermal X-ray continuum (Continumm fitting method)
2. Modeling the profile of the Fe K line (Fe K Method)
3. Quasi-Periodic Oscillations (QPO method)

3.2.1 Continuum Fitting Method

This method involves fitting the thermal continuum spectrum obtained from the accretion disk of a stellar black hole , to a relativistic thin disk model of the accretion disk developed by Novikov and Thorne(relativistic version of the Shakura and Sunyaev model), to obtain a_*. The dimensionless spin parameter (a_*) is related to the angular momentum of a spinning black hole by the relation,

$$a_* = \frac{cJ}{GM^2} \tag{3.5}$$

where, c is the speed of light, J is the angular momentum of the black hole, M is the mass of a black hole, G is the universal gravitational constant.

This method of spin measurement requires the knowledge of,

1. The distance D of the black hole binary,
2. The inclination angle i of the accretion disk(assumed to be same as the inclination of the binary system),
3. The mass M of the black hole.

Independently by other methods, the NT disk model predicts a certain profile for the radioactive flux $F(R)$ vs R where R is any radius in the disk, for a given mass M (mass of the blackhole), $\dot{M}$ (mass accretion rate) and spin parameter a_*,

$$F(R) = \frac{3GM\dot{M}}{8\pi R^3}\left(1 - \sqrt{\frac{R_{in}}{R}}\right) \tag{3.6}$$

It further assumes that the radius of the innermost stable circular orbit (R_{isco}) is same as the radius of the inner edge of the accretion disk(R_{in}) i.e. $R_{isco} = R_{in}$.

3.2.1.1 Measuring R_{in} and hence R_{isco}

Now, for measuring the inner edge of the accretion disk ($R_{in} = R_{isco}$ assumed for the Novikov Thorne model) we must then calculate the flux $F(R)$ and temperature $T(R)$ from the observed X-ray spectra of the disk. Since the emission spectra in thermal dominant state of the accretion disk is like a black body, we can easily calculate the flux $F(R)$ and effective temperature T_{eff} using the analogous equations that exist for a black body spectrum given by

For flux,

$$F(R) = \frac{3GM\dot{M}}{8\pi R^3}\left(1 - \sqrt{\frac{R_{in}}{R}}\right) = \sigma T_{eff}^4(R) \tag{3.7}$$

$$T_{eff}(R) = T_*\left(\frac{R_{in}}{R}\right)^{3/4}\left(1 - \sqrt{\frac{R_{in}}{R}}\right)^{1/4} \tag{3.8}$$

Thus knowing $F(R)$ and $T(R)$, we can calculate the solid angle $\nabla\omega$

$$\nabla\omega = \pi(\cos i)\left(\frac{R_{isco}}{D}\right)^2 = \left(\frac{\pi F}{\sigma T_{eff}^4}\right) \tag{3.9}$$

Now knowing the distance D and the inclination angle i we get the value of R_{in} from the above relation.

Now, there exists a monotonic relation between R_{isco}/M (where R_{isco} is the radius of the innermost stable circular orbit, M is the mass of the black hole) and spin parameter a_* given by, (Bardeen et al.)

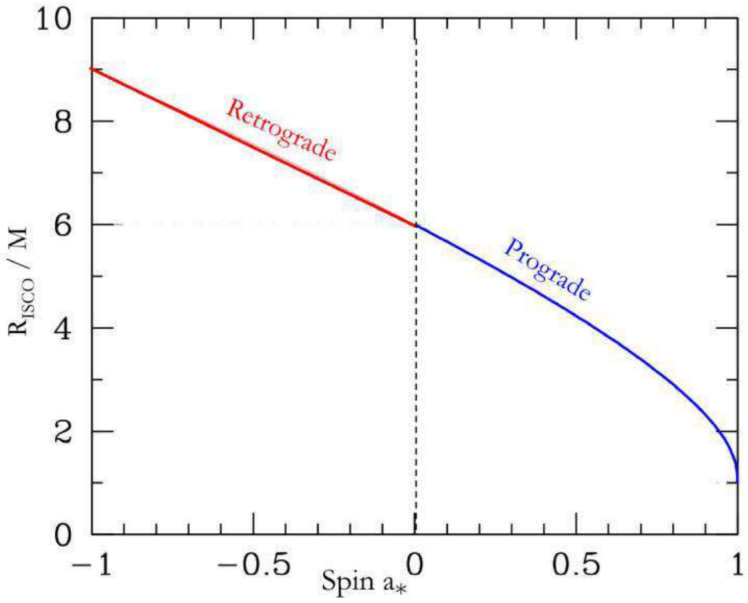

Figure 3.5: The relation between the ISCO radius and the black hole spin

Therefore, the idea is to measure the R_{isco} and finally R_{isco}/M (where M is obtained previously by another method), and thus with the aid of the graph above we can calculate the spin parameter a_*(Narayan et al.)

In reality, the accretion disk is an approximate black body, and we have to consider effects like electron scattering and therefore include a spectral hardening factor fcol thus giving us the true picture of the actual flux. Here,

$$f_{col} = \frac{T_{col}}{T_{eff}} \tag{3.10}$$

and

$$F(R) = \sigma\left(\frac{T}{f}\right)^4 \tag{3.11}$$

where, σ is the Stefan Boltzmann constant, T is the color temperature or T_{col}, F is the radiation flux, f is the spectral hardening factor or f_{col}.

3.2.2 Conditions for using the Novikov Thorne thin disk model

The disk flux goes to zero at R_{isco} and the accretion disk must be optically thick and geometrically thin i.e $H << R$ or L/L_{edd} <0.3, where H is the height of the accretion disk and at any radius R .

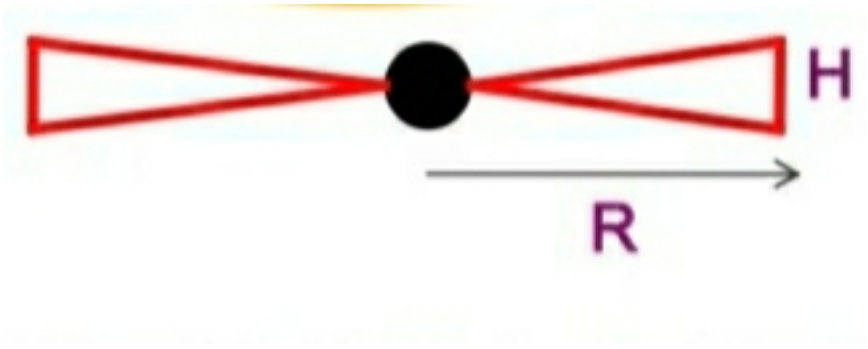

Figure 3.6: Diagram shows R and H of the accretion disk.

3.2.3 Fe K method

The fact that this method can be applied to both stellar mass and super massive black holes makes it one of the major methods to determine the spin of a black hole. In this method, we look at X-rays emitted by iron around a black hole. Some black holes show a characteristic iron emission line. Factors such as the Doppler shift caused by the rapid velocity of the iron in the accretion disk and gravitational red-shift caused by the intense gravity fields near the black hole broaden the line. By looking at the low-energy limit of the iron emission line, we can determine how close to the black hole the iron line emission took place and hence R_{isco} can be calculated.

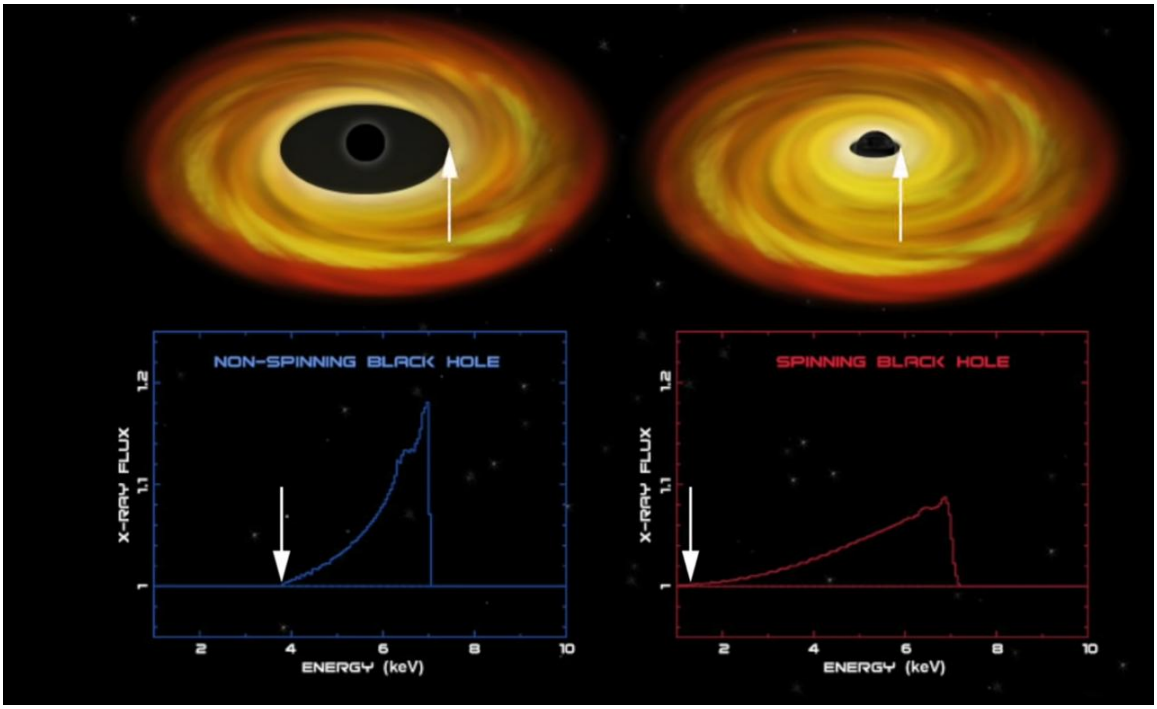

Figure 3.7: Low-energy limit: Spinning and non-spinning black holes

Most of the radiation from luminous accreting black holes is released within the innermost 20 gravitational radii (i.e., $20_{RG} = 20\frac{GM}{c^2}$). Iron is a major source of X-ray line

emission in such an energetic environment, with strong emission lines in the 6.4–6.9 keV band. Observations of such line emission give a diagnostic of the accretion flow as well as the behaviour of matter and radiation in the strong gravity regime near the black hole.[13] Disk lines have the advantage of not requiring the black hole's mass in order to measure spin, and other characteristics such as the inner disc inclination can be measured directly. These lines (and the larger disk reflection spectrum, of which iron lines are the most prominent part) have been utilised to determine general constraints on black hole spin in recent years. The value of dimensionless spin parameter a_* ranges from 0 to 1. [34] For stellar-mass black holes, in addition to the thermal disk component of emission (which is central to the CF method), a high energy power-law component of emission is always observed. This power-law component is dominant for supermassive black holes in active galactic nuclei (AGN) and it is thought to be produced by inverse Compton scattering of soft thermal photons in a hot (kT $\approx$ 100 keV) corona. Meanwhile, stellar-mass and supermassive black holes' discs are too cool (kT $\sim$1 and 0.01 keV, respectively) to produce the observed Fe K α emission line. Rather, this dominant line, and a host of other lines, are generated via X-ray fluorescence as a result of irradiation of the disk by the hard, coronal power-law component. The resulting complex spectrum is known as a "reflection spectrum." To use the Fe-line approach to estimate the spin, one must model the reflection spectrum in great detail. [33]

Using the inner disk as an indirect measure of the black hole spin parameter depends on two assumptions:

- "The accretion flow has a sharp transition from turbulent orbital flow to an inward plunging flow at (or close to) the innermost stable circular orbit." and,
- "The iron line emission has an inner truncation radius due to this transition in the flow properties."[34]

The spins of several stellar-mass and supermassive blackholes have been successfully measured using this method. The spin estimated for XTE J1550-564 (stellar black hole) using the Fe K method is $a_* = 0.55$, which is quite consistent with CF value. Also, the spins of several supermassive black holes have been reported which range from a_*=0.6 to > 0.98 . The most well studied of these is the Seyfert galaxy MCG-6-30-15. The 6.4 keV Fe Kα line of this AGCN is extremely broad and skewed.[33]

3.2.4 Quasi-Periodic Oscillations

The manner in which the X-ray light from an astronomical object flickers about certain frequencies is called quasi-periodic oscillations (QPOs). The X-rays in these situations are

emitted near the inner edge of an accretion disk in which gas swirls onto a compact object such as a white dwarf, neutron star, or black hole.

QPOs were identified in white dwarf systems first and then in neutron star systems. Initially, the neutron star systems found to have QPOs were of a class (Z sources and atoll sources) not known to have pulsations. As a result, the spin periods of these neutron stars were unknown. So that the gas does not fall mostly onto their magnetic poles, as in accreting pulsars, these neutron stars are thought to have relatively low magnetic fields. The accretion disk can get very close to the neutron star before being disrupted by the magnetic field because of its very low magnetic fields.

Quasi-periodic Oscillation is more or less periodic flux modulation near some frequency. Low-frequency QPOs are seen in low-hard and intermediate states and are strongly correlated with source spectral characteristics. QPOs are coupled with the non-thermal part of the spectrum. QPOs disappears in a soft state. Generally, QPOs show two or even three harmonics and sometimes a sub-harmonic.

3.2.4.1 Low-Frequency QPO

QPOs in BH and NS XRBs have been known for many years and have been divided into various classes. QPOs in BH XRBs are normally divided into two large groups, based on the frequency range where they are usually detected: the low-frequency QPOs and the high-frequency QPOs. The former is observed below $\sim 50Hz$, the latter are normally found above $\sim$ 100 Hz (but see the case of GRS1915+105, Belloni, et al., 2012) [1] and up to $\sim 500Hz$. [37]

- Type-A QPOs (see Fig. 3.8, top panel and 3.8, left panel) are the less common type of QPOs in BHBs. In the entire RXTE archive, only about 10 type-A QPOs have been found.

- Type-B QPOs have been seen in several BHBs and they appear during the SIMS, which is essentially defined on the presence of this QPO type. Type-B QPOs (Fig. 3.8, middle panel and Fig. 3.8) are characterized by a relatively strong ($\sim 4\%rms$) and narrow ($\nu/\Delta\nu \geq 6$) peak, which is found in a narrow range of centroid frequencies, i.e. around 6 Hz or 1-3 Hz (Motta et al., 2011b). At very low frequencies ($\leq 0.1Hz$), a weak red noise (a few percent rms or less) is detected. Sometimes together with a subharmonic peak, a weak second harmonic is often present. In some cases, the subharmonic peak is higher and narrower, resulting in a cathedral-like QPOs shape. [9]

- Type-C QPOs are by far the most common type of QPO in BHBs. Such types of QPOs can be detected pretty much in any spectral state (see Motta et al., 2012)

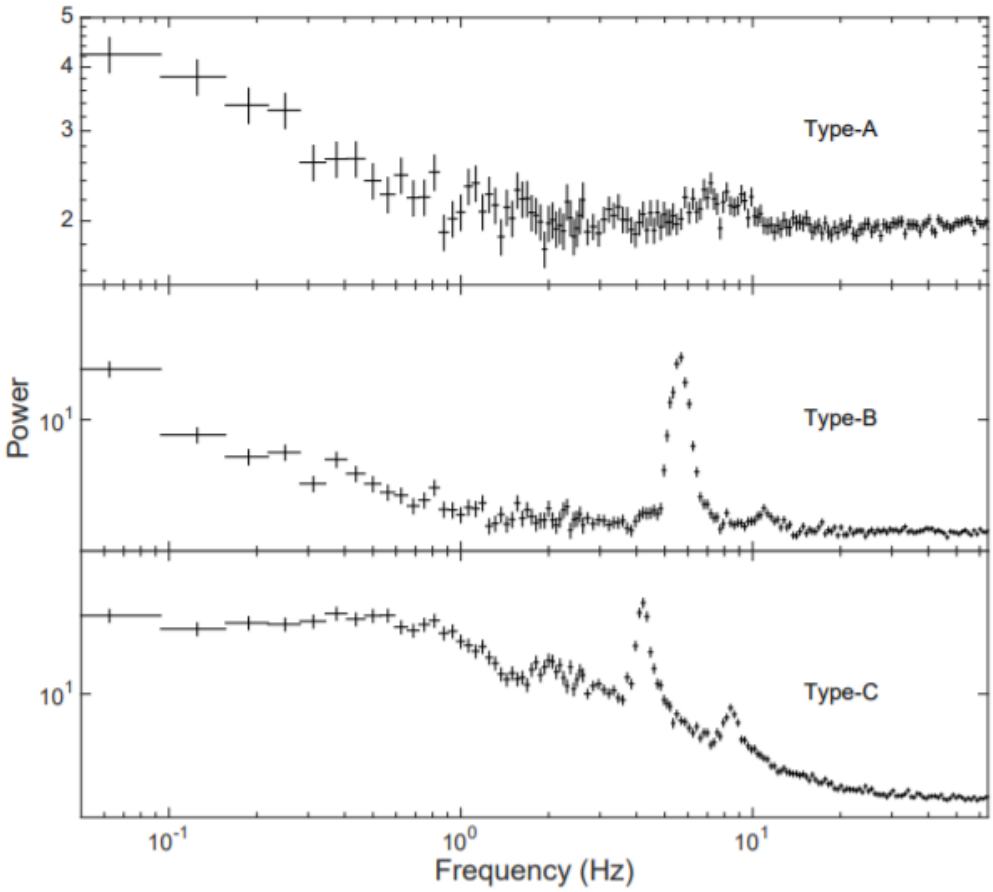

Figure 3.8: Examples of type A, B and C QPOs from our GX 339-4 observations. The centroid peak is indicated with an arrow. The contribution of the Poisson noise was not subtracted. Taken from Motta et al., 2011a.

3.2.4.2 High-Frequency QPO

The detection of the so-called KHz QPOs in NS binaries (see van der Klis, 2006) is among the most important discoveries that RXTE allowed. This result opened a window onto high-frequency phenomena in BHBs. The discovery of a transient oscillation at $\sim 67Hz$ (Morgan et al., 1997), the first high-frequency QPO (HFQPO) in a BHB was the result of the first observations of the very bright system GRS 1915+105. Since then, sixteen years of RXTE observations have yielded only a handful of detection in other sources (XTE J1550-564, GRO J1655-40, XTE J1859+226, H 1743-322, GX 339-4, XTE J1752-223, 4U 1630-47, GRS J1915+105, IGR J17091-3624), although, with a remarkably high number of detected high-frequency QPOs. [1] GRS 1915+105 seems to be an exception.

Models for HFQPOs:

- The relativistic precession model (RPM)
  The relativistic precession model, was originally proposed by Stella and Vietri, 1998, Stella et al., 1999 to explain the origin and the behaviour of the LFQPO and kHz

QPOs in NS X-ray binaries and later extended to BHs (Stella and Vietri, 1999, Motta et al., 2014a, Motta et al., 2014c)

- The warped disc model
  The HFQPOs are resonantly excited by specific disc deformations warps were stated by the warped disc model proposed by Kato, 2004a, Kato, 2004b. This model was generalized to include precession of the warped disk in Kato, 2005, and spin-induced perturbations were included in Kato, 2005. [25] [26]

- The nonlinear resonance model
  For this model, an assumption is made that non-linear 1:2, 1:3, or 2:3 resonance between orbital and radial epicyclic motion could produce the HFQPOs observed in both BH and NS binaries.

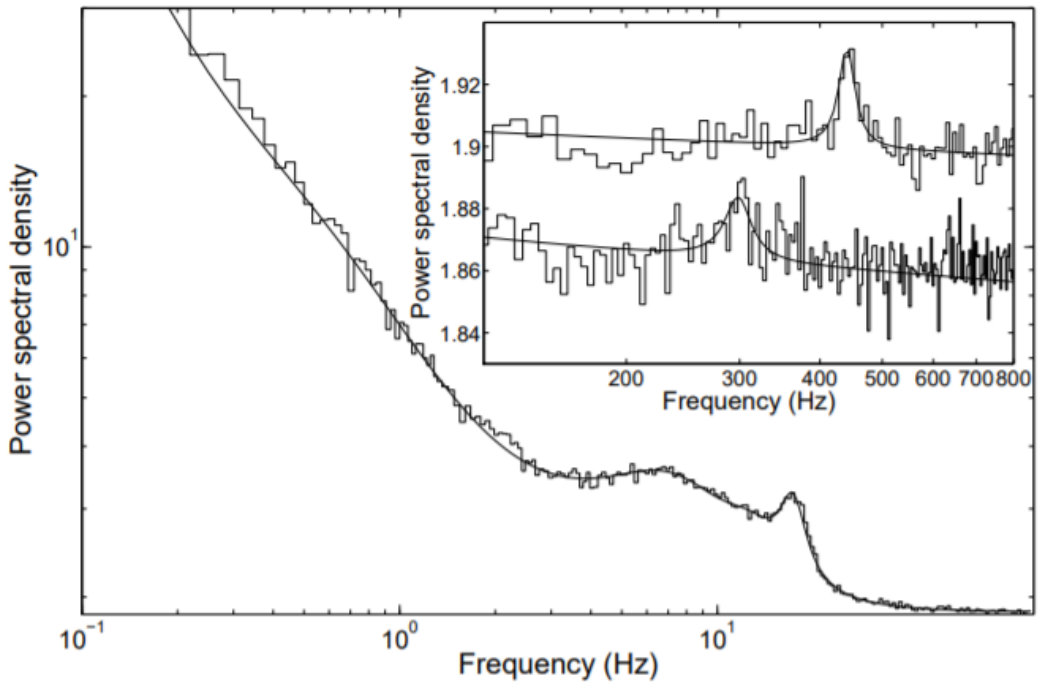

Figure 3.9: Power spectrum of GRO J1655-40 displaying three simultaneous QPO peaks (marked by arrows): the type C at $\sim 18Hz$, upper and lower high frequency QPO at ~ 300 and $\sim 450Hz$, respectively. From Motta et al., 2014a.

QPOs in particular provide a way to explore the accretion flow around BHs in ways that are inaccessible via energy spectra alone.

4

Different Stellar-mass BH candidates

4.1 CYGNUS X-1

Over three decades ago, Stephen Hawking placed and eventually lost, a bet against the existence of a black hole in Cygnus X-1. Today, astronomers are confident that the Cygnus X-1 system contains a black hole. In fact, a team of scientists has combined data from radio, optical, and X-ray telescopes including Chandra X-ray Observatory to determine the BH's spin, mass, and distance more precisely than ever before.

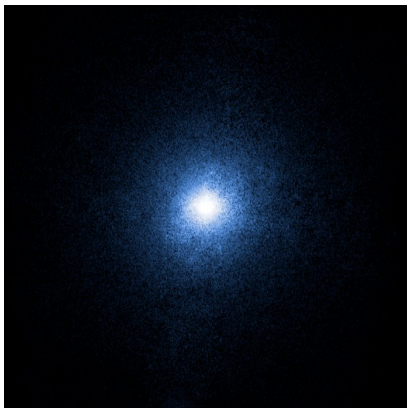

Figure 4.1: Chandra X-ray Observatory image of Cygnus X-1

With these key pieces of information, the history of the BH has been reconstructed. Thus, new information gives astronomers strong clues about how the BH was born, how

much it weighed, and how fast it was spinning.
Various methods through which its spin is determined and its value:[20]

1. Measurement of Spin via Fe K α Method:
   The round values of D, M, and i that Miller et al. used as input to KERRBB differ significantly from the paper of Jeffrey E. McClintock et al. [44], and these differences all serve to drive the spin-down, e.g., using Miller et al. values of these parameters and Jeffrey E. McClintock et al. spectrum (which gives the lowest value of spin), we find $a_* = 0.74 \pm 0.01$.

2. Measurement of Spin via QPO Model:
   In this model, the QPO is produced as a result of emission from an orbiting bright spot that is undergoing relativistic nodal and periastron precessions in a slightly tilted and eccentric orbit. The spin parameter is predicted to vary with mass as $a_* \propto M^{\frac{-1}{5}}$. [2] And therefore, the corrected value of spin is $a_* = 0.43$ for our adopted black hole mass M = 14.8 $M_\odot$. The large discrepancy between this moderate value of spin and the extreme value we find maybe a consequence of a fundamental assumption of their model, namely, that the black hole is rotating slowly $(a_* << 1)$. On the other hand, the precession model, with its assumption of geodesic motion, may not apply in this instance.

3. An Alternative Dynamical Model:
   An alternative model has been used which assumes synchronous rotations. This alternative model gives a poor fit to the data $(\Delta\chi^2 \approx 13)$, and it results in disharmony between the light curve and velocity data on the one hand, and the radius and rotational velocity of the O-star on the other. Because of this disharmony, the uncertainties in M and i for the previous model are significantly larger than those for our favored model, although the central values of these parameters differ only modestly: $M = 15.8 \pm 1.8\, M_\odot$ and $i = 28.5^\circ \pm 2.2^\circ$. Using these values for the alternative model and spectrum (which gives the lowest value of spin), the error analysis has been repeated and obtained the following 3σ lower limit on the spin parameter: $a_* > 0.92$.

4. Alignment of Spin and Orbital Angular Momentum:
   In recent population synthesis studies predict that the majority of systems will have rather small (10°) misalignment angles (Fragos et al. 2010).[15] Another point is, in the case of Cygnus X-1, there is reason to believe that the misalignment angle is especially small because of the binary system's low peculiar velocity, which indicates that the system did not experience a large "kick" when the black hole formed. [44] Even if there exists a misalignment angle as large as, e.g., 16°, the spin value is still $a_* > 0.95$.

Various methods through which its mass is determined and its value: [42]

1. By an extensive collection of optical photometric and spectroscopic data taken from the literature:
   The black hole mass of $M = 14.8 \pm 1.0\ M_{\odot}$, a companion mass of $M_opt = 19.2 \pm 1.9\ M_{\odot}$, and the angle of inclination of the orbital plane to our line of sight of $i = 27.1 \pm 0.8^{\circ}$.

2. Analysis of optical spectral line profiles:
   The observed mass was in the range $8.2 \leq M \leq 12.8\ M_{\odot}$ from their analysis.

3. X-ray spectral/timing data and a scaling relation based on the dynamically determined masses of three black holes:
   The observed mass was in the range $7.9 \leq M \leq 9.5\ M_{\odot}$ from their analysis.

4. Examination of high-resolution, ultraviolet (UV) spectroscopy from Hubble Space Telescope of the photospheric spectrum of the O-supergiant in the massive X-ray binary HD 226868 = Cyg X-1: [5]
   The observed mass was in the range $8 \leq M \leq 16\ M_{\odot}$ from their analysis.

4.2 4U 1543-47

4U 1543-47 is a low-mass X-ray binary that harbours a stellar-mass black hole located in our Milky Way galaxy. It is in the constellation Lupus having alternate name as IL Lupi. Once every decade or so, the star system 4U 1543-47 erupts, producing a powerful torrent of X-rays. The first eruption was recorded by the Uhuru X-ray satellite in 1971, with subsequent bursts in 1983, 1992, and 2002. At its maximum, the system shines up to 20 million times brighter in X-rays during these outbursts than during the years-long quiet time between them.

The accretion disk's magnetic field funnels some of the superhot gas, known as plasma, into "jets" of charged particles that shoot into space from the black hole's north and south poles. As compared to many other erupting black holes, the jets from 4U 1543-47 are shorter and weaker.
Different methods through which spin is determined and its value:

1. Simultaneous fitting the thermal disk continuum and by modelling the broadened Iron k-shell emission lines and additional blurred reflection [35]
   Using a combination of continuum-fitting, and disk reflection modeling, we have measured the spin to be $a_* = 0.43^{+0.22}_{-0.31}$.
   Prior works measuring the spin of 4U 1543-74 which used both of these methods

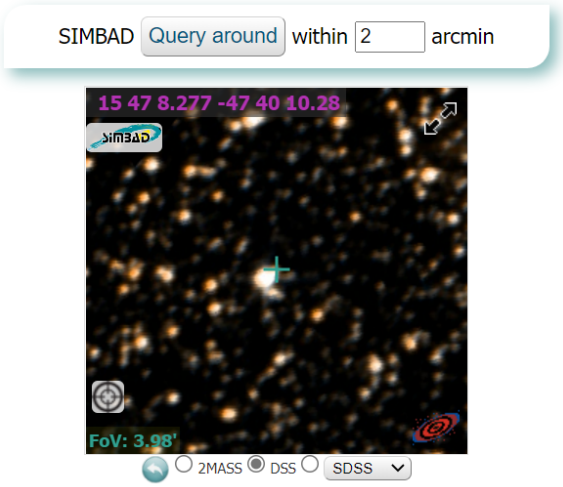

Figure 4.2: 4U 1543-475 by DSS

separately had found conflicting values of a_* (0.75–0.85 by Shafee et al. 2006; 0.3 ± 0.1 by Miller et al. 2009). Our measured spin is lower than that obtained by Shafee et al. (2006) [47], primarily because they assumed that the binary inclination is equal to the inclination of the disk.

2. X-ray reflection spectra and made a joint-fit to these spectra with relxill for the reflected emission [12]
   The spin parameter a_* is obtained to be $0.67^{+0.15}_{-0.08}$. As to its spin parameter, Shafee et al. (2006) first reported its spin with the continuum-fitting method. They estimated its spin to be 0.8 ± 0.1. Then, Miller et al. (2009) and Morningstar & Miller (2014) reported two spin measurements $a_* = 0.43^{+0.22}_{-0.31}$, 0.3 ± 0.1 and , respectively, both constrained by combining the continuum-fitting and the X-ray reflection fitting methods. These three works utilized the previous mass of $9.4 \pm 1.0\, M_\odot$ and distance of 7.5 ± 1.0 kpc, which were reported in Park et al. (2004). Except that Miller et al. (2009) used the inclination angle of $32^{+3\circ}_{-4}$ constrained by their own fits to the iron line, the other two works used the inclination angle of $20.7 \pm 1.5^\circ$, which is equal to the binary orbital inclination angle.

4.3 SS433

SS 433 is one of the most unconventional star systems ever discovered. It is an eclipsing X-ray binary system in the Milky Way galaxy, with the primary being a stellar-mass black hole.

The first micro quasar discovered was SS 433. SS 433, also known as V1343 Aquilae, is in the galactic plane at 5.5 kpc (l= 39.7° and b= -2.2°). SS433 is a close binary system

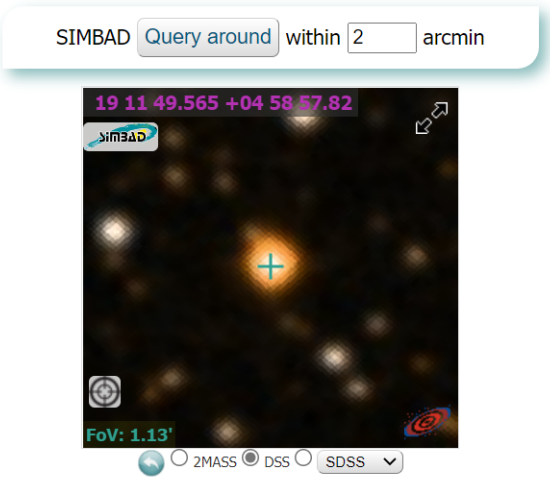

Figure 4.3: SS433 by DSS

with a 13.1-day orbital period. The existence of narrow oppositely directed sub relativistic jets emitting red and blue-shifted, periodically variable lines distinguishes this source. According to a widely accepted model of this object, a continuous regime of supercritical gas accretion onto the relativistic star is maintained. As a result, a supercritical accretion disc forms, along with narrow jets of gas propagating perpendicular to the disc plane from the disk's central regions at the relativistic speed of $0.26c$. The optical star fills its critical Roche lobe, allowing a powerful and nearly continuous flow of gas into the relativistic star's region at a rate of $\simeq 10-4M_{\odot}$/yr.

Different methods through which mass is determined and its value:

1. Parameters derived from ellipsoidal study and spectroscopic data: [11]
   The observed mass was in the range 6 - 20 $M_{\odot}$ from their analysis.

2. The emission spectra of the circumbinary disk & inference from the stability of the period of the binary orbit: [4]
   The observed mass was found to be 15 $M_{\odot}$.

4.4 V4641 Sagittarii

With a distance of only 1,600 light-years, V4641 Sagittarii (Sgr) was thought to be the closest black hole to Earth. However, continued observations of the system have pushed it out to several times that distance at least 24,000 light-years. V4641 Sgr is made up of a black hole and a "typical" companion star. The companion's hot gas is being stolen by the black hole. When enough gas accumulates in a disc around the black hole, a large outburst occurs, causing the system to shine much brighter than usual. Because a large portion of

the extra energy is in the form of X-rays, V4641 is classified as an X-ray nova. It was discovered by detection of its jet.

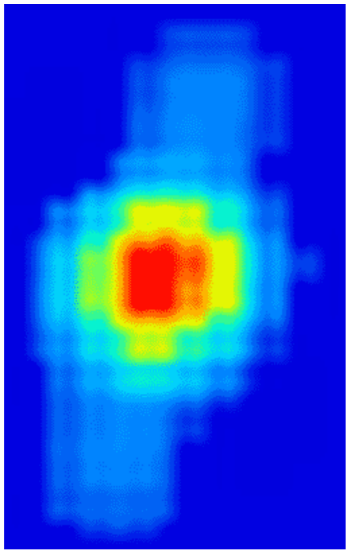

Figure 4.4: V4641 Sgr imaged just after emitting an outburst in the radio band. Jets, which lasted only minutes, are visible. Image: VLA.

This could be the first black hole that we travel to when we finally break free of our solar system. Or, to hear astronomers talk about it, it could be merely one stop on a visit to many of our black hole neighbours.
Spectroscopic method was used to determine the mass if found to be at least 8.7 $M_{\odot}$,and inclination is found to be in the range $72.3^{\circ} \pm 4.1$, a mass ratio of Q = 2.2, component masses for the system of $M_{BH} = 6.4\ M_{\odot}$and $M_2 = 2.9\ M_{\odot}$ and radius is roughly equal to 18-60kms. [31]

4.5 LB-1

The binary star system LB-1 is located in the constellation Gemini. Outside of ordinary single stellar evolution parameters, it was concluded that the system contained a "monster" black hole. The star's undiscovered companion was discovered by measuring the radial velocity shifts of its companion star. If it is a black hole, it would be the first time a stellar black hole has been discovered without the use of X-ray emissions. If the distance from parallax is ignored and the star is assumed to be an ordinary main sequence B-type star, the unseen companion LB-1 B or LB-1 * could be a black hole with a mass of about 70 solar masses, which is more than twice the mass predicted by most current stellar evolution theories. It would be in the stellar-mass black hole range, less than intermediate-mass black holes in size.

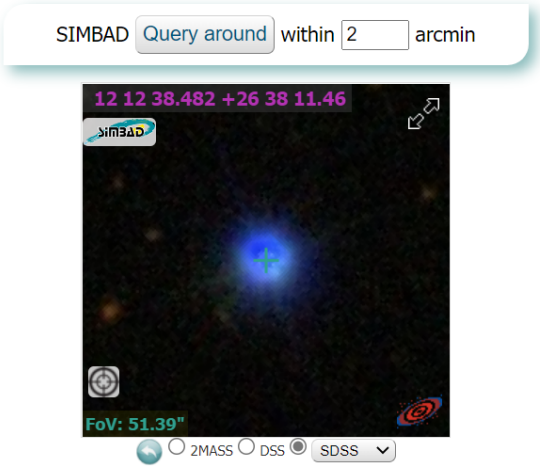

Figure 4.5: LB-1 by SDSS

A 70 $M_{\odot}$ BH could form if a "normal" stellar-mass BH merges into the core of a & 60 $M_{\odot}$ during common-envelope evolution, followed by the massive star accreting onto its BH core. One intriguing possibility is that the dark mass still contains two BHs, which are orbiting each other in an inner binary, with the observed star as a tertiary companion. Individual BH masses approaching 35 $M_{\odot}$ are required, posing less of a challenge for their formation. In this case, the system would serve as a testing ground for the formation of binary BHs in triple systems. Using the $H\alpha$ emission line comparison, the mass of the BH is found to be 68 $M_{\odot}$ and the inclination is $15 - 18°$. [30]

4.6 Cygnus X-3

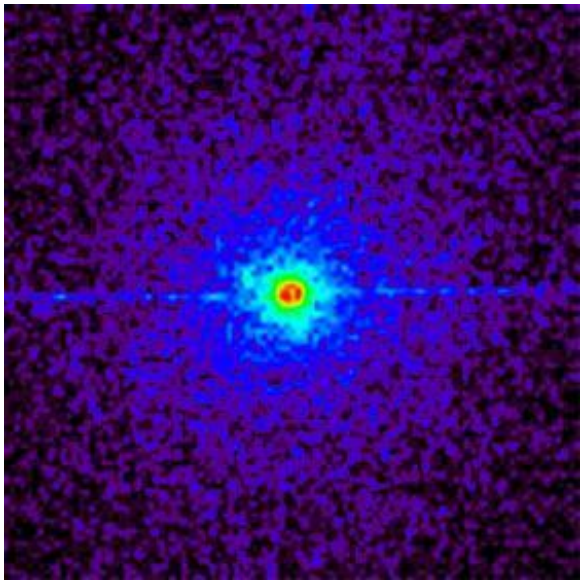

Figure 4.6: Cygnus X3 and its X-ray halo

Cygnus X-3 is a high-mass X-ray binary (HMXB), which is one of the most powerful binary X-ray sources in the sky. It is frequently thought to be a micro quasar, and it is thought to be a compact object in a binary system that is attracting a stream of gas from an ordinary star companion. It is one of only two HMXBs known to contain a Wolf-Rayet star. It is not visible to the naked eye, but it can be seen at radio, infrared, X-ray, and gamma-ray wavelengths.

Cygnus X-3 is also notable for being the only micro quasar firmly detected in high energy gamma rays with energies greater than 100 MeV.

Mass of this BH is found by orbital analysis which is less than 5 $M_{\odot}$, probably around 2 $M_{\odot}$. [27]

4.7 XTE J1118+480

The Ursa Major binary XTE J1118+480 is a low-mass X-ray binary. It is a soft X-ray transient containing a black hole and is most likely a micro quasar. The compact object in XTE J1118+480 has a mass greater than 6 $M_{\odot}$, indicating that it is not a neutron star. The characteristics of XTE J1118+480's radio emissions indicate that it is a micro quasar.

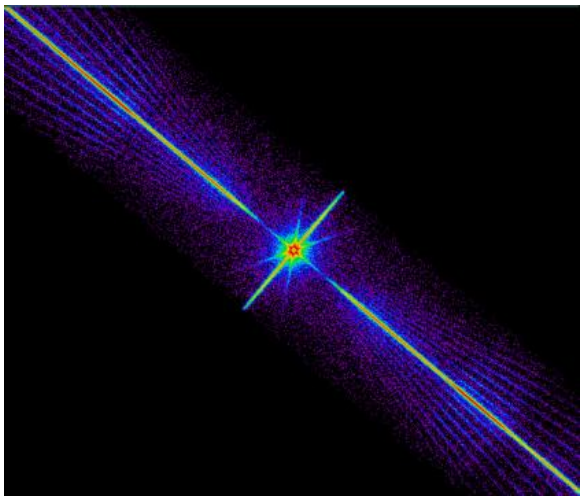

Figure 4.7: XTE J1118+480: by Chandra X-ray Telescope

Surprisingly, the companion star has a metal-rich composition that includes magnesium, aluminium, calcium, iron, and nickel. Because of this observation, the black hole was most likely formed by the supernova of a metal-rich star rather than the direct collapse of a massive star. Because a supernova would likely eject the companion from the system, the two objects in the binary system were most likely not born together. The most likely explanation for how XTE J1118+480 became a part of the binary system is that it formed in the central galactic halo.

Mass: $8.53 \pm 0.6\ M_{\odot}$ [8] and $8.30^{+0.28}_{0.14}\ M_{\odot}$

Spin: in the range 0.29-0.59
Inclination: $68^{+2.8}_{-2}$ and 68-79

4.8 V404 Cygni

V404 Cygni is one of the most accurately weighed black holes. In 1989, the Japanese X-ray astronomy satellite Ginga found a burst of X-rays from an object labelled at the time GS2023+338. It was soon realized that the X-rays were, in fact, coming from alongside a star which had been seen as a nova in 1938. As per optical records, the old nova had brightened considerably at the same time that the burst of X-rays was observed. This confirmed the fact that they came from the same source. The burst of X-rays was too strong to be explained in terms of the presence of a white dwarf in a recurrent nova, so they had be coming from a neutron star or a black hole.

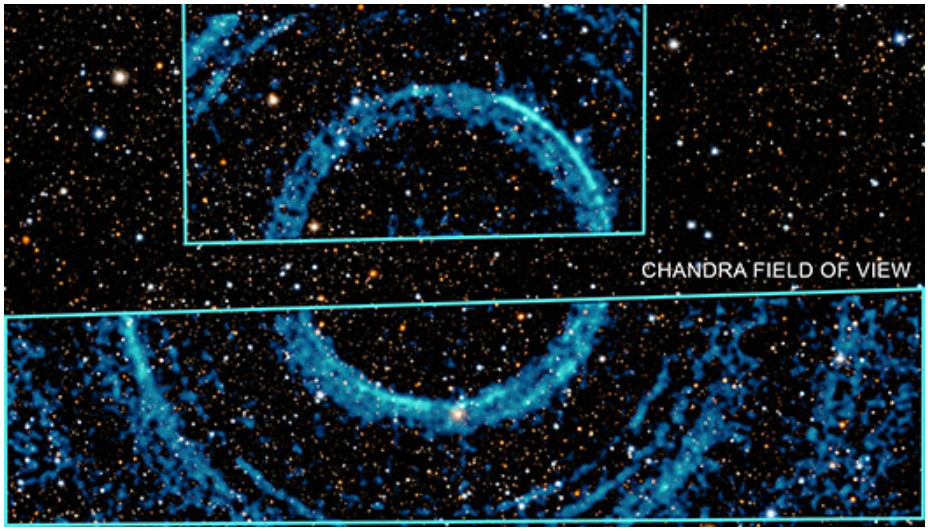

Figure 4.8: V404 Cygni: Huge Rings Around a Black Hole

It is much easier to study than other black hole candidates because V404 Cygni is relatively close to us. Over the next few years, V404 Cygni was investigated in great detail, and by late 1994 astronomers using the **William Hershcel Telescope** and the **UK Infrared Telescope** had enough information to pin down the properties of the two stars in this binary system. With a speed of 210 kilometres per second, the visible star orbits an unseen partner once every 6.5 days. The orbital details reveal that the unseen companion is seventeen times the mass of the visible star. The final piece of the puzzle fell into place when observers were able to estimate the angle at which the visible star's orbit is tilted on the sky, revealing that the two objects' real masses are 0.7 and 12 solar masses, respectively. The visible star is the lighter object, implying that the unseen companion has twelve times the mass of our Sun, or nearly four times the Oppenheimer-Volkoff limit for the greatest

conceivable mass for a neutron star. It has to be a black hole, and is the closest one to our Solar System that we know of. The mass and inclination for this BH is 12 $M_{\odot}$ and 60 degrees (Upper limit) respectively.[21]

4.9 LMC X1

It is the first extra galactic black hole binary to be discovered. It is located in the large megallanic cloud at a distance of 48.10 ± 2.22 kpc (Orosz et al.) and has a O III giant as the companion. Moreover, it is a persistent source of X-rays i.e. it emits X-rays throughout unlike other black holes that are transient that switch between their high and soft states. Observations until now have revealed it to be always in its high soft state with a luminosity of $L_{bol} \approx 2.210^{3}8$ erg s^{1} (Long et al. 1981). It has a mass of 10.91 ± 1.41 $M_{\odot}$ (Orosz et al. 2009).

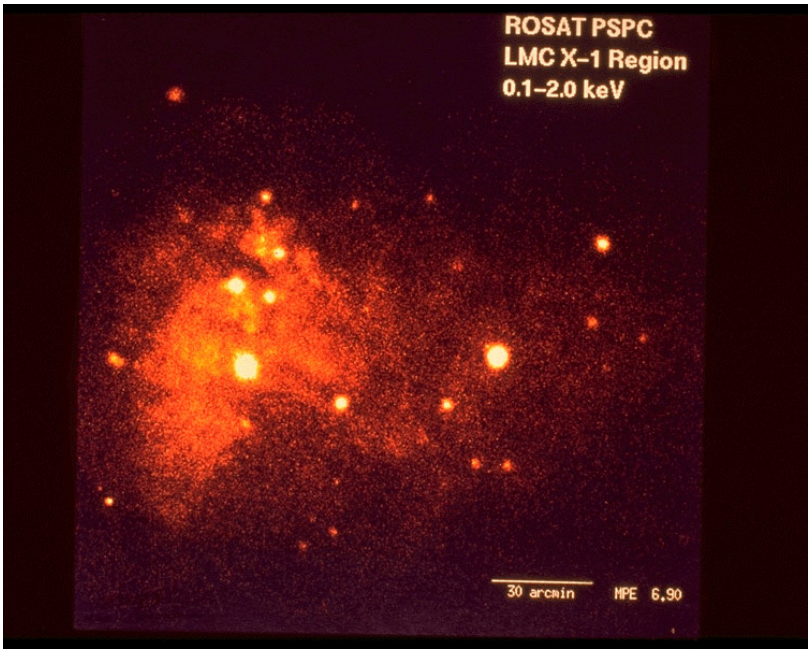

Figure 4.9: An X-ray view shows the region around LMC X-1 (bright area at left). X-rays from the black hole's accretion disk cause clouds of gas around the system to emit their own X-rays. [ROSAT/MPE/NASA]

Methods used for calculating the spin:

1. Continuum fitting method: It is a good source for the x ray continuum fitting method to be used to calculate its spin as it is not along the plane of our galaxy thus avoiding the large amount of absorption of soft x rays, thus giving us a good spectra. Also it has well established values for its mass, spin and distance which is a necessity for this method.

Previous estimates of its dimensionless spin parameter a_* by this method have been calculated by Gierlinski et al. (2001) but it was not accurate as Mass inclination and distance were not well established then. Gou et al.(2009) and Tripathi et al.(2020) also attempted to calculate a* using various relativistic models to fit the x ray spectra obtained from observations. Gou et al. used KERRBB, SIMPL, and PHABS to fit the thermal component, the comptonised component and account for interstellar absorption respectively and arrived at a value of $a_* = 0.92^{+0.05}_{-0.07}$. Tripathi et al used a different model 'nkbb'(Zhou et al.2019) , simpl and tbabs respectively for the thermal , comptonised componentand galactic absoption respectively,and fixed the value of f(spectral hardening factor) of 1.55 and values for mass , inclination and distance given by Orosz et al. and arrived at $a_* = 0.998_{-0.004}$.

Mudambi et al used $f = 1.7$ (Shakimura and Takahara) and values for mass , distance and inclination given by Orosz et al. and estimated $a_* = 0.93^{+0.01}_{-0.01}$ and $0.93^{+0.04}_{-0.03}$.

2. Fe line method: Steiner et al used this method to calculate $a_* = 0.97^{+0.01}_{-0.13}$ and $0.97^{+0.02}_{-0.25}$ using models refbhb and ireflect.

4.10 A0620-00

A0620-00 was discovered as an X-Ray nova on the 3rd day of August 1975. Boley et al.1976 [3], observed it along with a mag 12 star. McClintock & Remillard 1986[32], proposed a mass function of $3.18 \pm 0.16\ M_\odot$ and a $3.20\ M_\odot$ which is a lower limit to the mass of the relativistic compact object in the system. This was proposed with 3 sigma. This result makes A0620-00 a potent stellar mass black hole.

However, the accurate mass measurement of the black hole remains dominated by uncertainties, which can be solved by knowing the precise value of the inclination angle (i). Please refer to chapter 3 for more information on this. Over the years, many attempts were made by various groups to measure the value of the inclination angle (i) by fitting the ellipsoidal light curves. But, their results show wide discrepancies. For instance, an angle of inclination of 62° was given by Haswell et al. (1993)[22], Shahbaz et al. (1994) [48] showed an inclination of 36.7° while Gelino et al. (2001) [19] showed an inclination of 48°. A huge range of inclinations was proposed by Froning & Robinson (2001) [17] ranging from 38° to 75°. Gelino and other proposed mass of $11.0 \pm 1.9\ M_\odot$ with an orbital inclination of $40.75 \pm 3^\circ$ and mass ratio $q = 0.067 \pm 0.01$ [19]. Froning and Robinson found a mass in the range $3.3 \leq M \leq 13.6\ M_\odot$ [17] Froning and Bitner have proposed a mass of $9.7 \pm 0.6\ M_\odot$ [18].

These discrepancies and disagreements are caused by mainly two factors which are as follows,

- Changes in the light curve
- Uncertainty regarding the contribution of the disk in the no-nellipsoidal variability

Changes in the light curve: The light curves of the system have changed repeatedly over the years. The above was studied and shown by Leibowitz et al. (1998).[29] Hence, various attempts have resulted in inconsistent values. However, Cantrell et al.(2008) have shown that the system remains very stable with minimum flaring episodes. This state of minimum flaring and stability is termed as passive state and during this state, the system gets relatively redder. Cantrell and others studied and analysed light curves while the system was in its passive state and showed no aperiodic variabilities and had a consistent curve. They came up with an inclination angle higher than 10° estimated by previous studies.
Disk contribution: The inclination angle (i) calculated from the light curves is subjected to the assumptions made regarding the disk fraction while making a fit. Disk fraction is defined to be a ratio of the disk flux to the total flux. An argument stating the lack of the disk fraction in the NIR region was proposed by some authors (Gelino et al. (2001)).[19] However, Froning and others have found a significant NIR disk fraction.[18] Following works have shown that the disk fraction is very variable. Therefore, a better study on the role of disk fraction is very crucial in order to calculate the inclination angle hence the mass.

Cantrell et al.(2010) have estimated an inclination angle of $51 \pm 0.9^{\circ}$ and a Mass of $6.6 \pm 0.25\, M_{\odot}$. You et al. (2010) found the dimensionless spin parameter a_* of 0.12 ± 0.19.

4.11 GRO J1655-40

GROJ1655-40 is a binary star in the constellation of Scorpius that consists of F type star i.e a star with a mass 1.0 to 1.4 times the mass of the sun, this is a low mass X-ray binary. It is considered to be a microquasar since it generates a lot of energy in a little amount of space. This black hole reported first successful attempt at collecting precise simultaneous measurements of a black hole's mass and spin in a binary system, with the help of RXTE observations. The outburst was discovered to have QPOs i.e Quasi-periodic oscillations. [36]

Black hole -Xray binaries have black hole accreting material from a companion star, the accreting material reaches very high temperature such that it emits X-Rays providing us a means to study the accretion flow. The light emitted from the accretion disc oscillates rapidly, and the way in which this X-ray flickers are called QPOs. Quasi-periodic oscillations originate in the innermost regions of the accretion flow. In a Power Density Spectrum

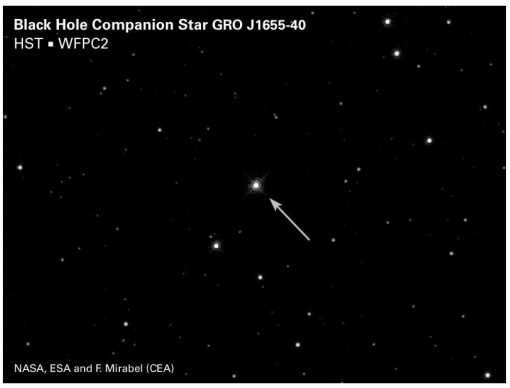

Figure 4.10: ESA, NASA, and Felix Mirabel (French Atomic Energy Commission and I nstitute for Astronomy and Space Physics/ Conicet of Argentina)

(PDS), they take the form of narrow peaks with certain centroid frequencies that can be associated with motion in the strong gravitational field.

QPOs are divided into two types: low-frequency Quasi periodic oscillations (LFQPOs) which have a centroid frequency of $\leq$30 Hz and high-frequency Quasi periodic oscillations (HFQPOs) which have a centroid frequency of $\geq$60 Hz. LFQPOs are commonly found whereas HFQPOs are rare. Only GROJ1655-40 could report two simultaneous HFQPOs which are called lower and upper HFQPO. LFQPOs are further classified as type A, type B, and type C. Many Models using G.R. and fundamental frequencies of motion have come up to explain the origin and physical nature of QPOs. One such model is relativistic precision model (RPM). The RPM, when applied to X-ray high time resolution data of BH binaries, provides an independent method for measuring the mass and spin of a BH at the same time, using just X-ray timing. QPOs tend to be present in every spectral state in the hardness Intensity diagram i.e in hard, intermediate and soft states. Different accretion rates can be tracked using hardness intensity diagram (HID) . Hardness is defined as the ratio of the counts in a harder X-ray band to soft X-ray band. In RPM certain combinations of fundamentals frequencies of motion in strong gravitational field are associated with frequency of QPO observed in accreting compact bodies. Frequencies of motion here are orbital frequency in equitorial plane which is associated with upper HFQPO, periastron precision frequency is associated with lower HFQPO and nodal precision frequency is associated with LFQPO here it is type C. We considered three energy bands for our analysis: 1.51– 27.40 keV, 1.51–9.52 keV and 9.52-27.40 keV.

Two different samples of observations are defined in a paper.[36]

SAMPLE A: Only the observations whose PDS indicated a low-frequency characteristic that could be characterised as a type-C QPO were included in Sample A. SAMPLE B: Only observations with high frequency features in their PDS were included in Sample B. Then they compared the two samples to see if there were any observations that showed both high

frequency QPOs and type C QPOs. Which are divided into B_1 and B_2 sub-samples. They have three observations in sub sample B_1: a low-frequency type C QPO at 17 Hz that can be detected in soft, hard, and int total energy bands, an HFQPO at 300 Hz that can be detected in soft band, and an HFQPO at 440 Hz that can be detected in hard band.
In QPO model, the frequency of certain QPOs observed in accreting compact objects is linked to particular combinations of fundamental motion frequencies in the strong field regime. When motion occurs in the equatorial plan, the orbital frequency measured by a static observer at infinity can be calculated using the geodesic equation:
The epicyclic frequency ν_r and in the vertical direction, the vertical epicyclic frequency ν_θ are given by:

$$\nu_\phi = \pm\frac{1}{2\pi}\left(\frac{M}{r^3}\right)^{\frac{1}{2}}\frac{1}{1\pm a\frac{M}{r}^{\frac{3}{2}}} \tag{4.1}$$

$$\nu_r = \nu_\phi\left(1-\frac{6M}{r}-3a^2\left(\frac{M}{r}\right)^2\pm 8a\left(\frac{M}{r}\right)^{3/2}\right)^{1/2} \tag{4.2}$$

$$\nu_\theta = \nu_\phi\left(1+3a^2\left(\frac{M}{r}\right)^2\mp 4a\left(\frac{M}{r}\right)^{3/2}\right)^{1/2} \tag{4.3}$$

These three coordinate frequencies lead to two additional frequencies, the periastron precession frequency $\nu_{per} = \nu_\phi - \nu_r$ and the nodal precession frequency $\nu_{nod} = \nu_\phi - \nu_\theta$. The orbital frequency ν_ϕ is related with the upper HFQPO in the RPM, while the periastron precession frequency ν per is associated with the lower HFQPO. Under the assumption that nodal precision frequency, orbital frequency and periastron precision frequency arise from the same distance or radius from the black hole. By the above equations, it can be understood that these frequencies depend on mass, spin parameter and radius at which QPOs are produced.
Assuming these frequencies being produced from the same distance we get three simultaneous equations, this system of equations is then solved using Newton method.

- They calculate radius at which the corresponding QPO is produced for every single possible mass spin pair in the given range, here the range is about 3 – 50 solar masses and spin 0-1.
- Now after that they got three sets of mass spin radius solutions one for each RPM equation.

- Here they mentioned a method called monte carlo method through which they simulated 10^5 sets of three frequency based on PDS of GRO J1655-40.
- They solved the RPM system for each set of three simulated frequencies following steps and obtained three distributions of mass, spin and radius values (105 values for each distribution) consistent with being Gaussian-distributed.
- They distribution of mass, spin and radius obtained in step $M = (5.31 \pm 0.07)\ M_{\odot}$, $a_* = 0.290 \pm 0.003$, $R = (5.68 \pm 0.04) R_g$.

They've shown that when three QPOs (two high-frequency and one low frequency) are found in the X-ray light curves of a BH binary, their frequencies can be used to solve the RPM's functional form, which is entirely dependent on the compact object's mass and spin, as well as the radius at which the orbiting matter gives rise to the QPOs.
They calculated a mass of $5.31 \pm 0.07\ M_{\odot}$, which is fully consistent with the value of the mass determined independently through spectro-photometric optical observations $M_{opt} = 5.4 \pm 0.3\ M_{\odot}$.
Previous estimates of the spin of the BH in GRO 1655–40 were based on X-ray spectral analysis and gave higher, and yet different, values a_* = 0.65– 0.75, a_* = 0.94–0.98.
They found a mass (M = $(5.31 \pm 0.07)\ M_{\odot}$) that matches the value obtained from optical research perfectly. The spin we get (a_* = 0.290 ± 0.003), on the other hand, is inconsistent with estimations from either the Fe K line approach or the spectral continuum method modelling.

5
Conclusion

We have studied certain number of black hole candidates. And noted the values of the fundamental parameters for each stellar mass black hole which has been determined through various methods. It has been observed that for a particular candidate there are multiple values of the same parameter through different methods, be it for spin or mass. The reason for such discrepancies have been mentioned if available

Refrences

[1] D. Altamirano and T. Belloni. Discovery of high-frequency quasi-periodic oscillations in the black hole candidate igr j17091–3624. *The Astrophysical Journal Letters*, 747(1):L4, 2012.

[2] M. Axelsson, L. Borgonovo, and S. Larsson. Evolution of the 0.01–25 hz power spectral components in cygnus x-1. *Astronomy & Astrophysics*, 438(3):999–1012, 2005.

[3] F. Boley, R. Wolfson, H. Bradt, R. Doxsey, G. Jernigan, and W. Hiltner. Optical identification of a0620-00. *The Astrophysical Journal*, 203:L13, 1976.

[4] M. Bowler. Ss 433: Two robust determinations fix the mass ratio. *Astronomy & Astrophysics*, 619:L4, 2018.

[5] S. Caballero-Nieves, D. Gies, C. Bolton, P. Hadrava, A. Herrero, T. Hillwig, S. Howell, W. Huang, L. Kaper, P. Koubskỳ, et al. The ultraviolet spectrum and physical properties of the mass donor star in hd 226868= cygnus x-1. *The Astrophysical Journal*, 701(2):1895, 2009.

[6] A. G. Cantrell, C. D. Bailyn, J. E. McClintock, and J. A. Orosz. Optical state changes in the x-ray-quiescent black hole a0620–00. *The Astrophysical Journal Letters*, 673(2):L159, 2008.

[7] A. G. Cantrell, C. D. Bailyn, J. A. Orosz, J. E. McClintock, R. A. Remillard, C. S. Froning, J. Neilsen, D. M. Gelino, and L. Gou. The inclination of the soft x-ray transient a0620–00 and the mass of its black hole. *The Astrophysical Journal*, 710(2):1127, 2010.

[8] J. Casares and P. G. Jonker. Mass measurements of stellar and intermediate-mass black holes. *Space Science Reviews*, 183(1-4):223–252, 2014.

[9] P. Casella, T. Belloni, J. Homan, and L. Stella. A study of the low-frequency quasi-periodic oscillations in the x-ray light curves of the black hole candidate xte j1859+ 226. *Astronomy & Astrophysics*, 426(2):587–600, 2004.

[10] J. M. Corral-Santana, J. Casares, T. Munoz-Darias, F. E. Bauer, I. G. Martinez-Pais, and D. M. Russell. Blackcat: A catalogue of stellar-mass black holes in x-ray transients. *Astronomy & Astrophysics*, 587:A61, 2016.

[11] D. Crampton and J. Hutchings. The ss 433 binary system. *The Astrophysical Journal*, 251:604–610, 1981.

[12] Y. Dong, J. A. García, J. F. Steiner, and L. Gou. The spin measurement of the black hole in 4u 1543-47 constrained with the x-ray reflected emission. *Monthly Notices of the Royal Astronomical Society*, 493(3):4409–4417, 2020.

[13] A. Fabian. Strong field gravity and spin of black holes from broad iron lines. *Black Holes*, 21:182, 2011.

[14] W. M. Farr, N. Sravan, A. Cantrell, L. Kreidberg, C. D. Bailyn, I. Mandel, and V. Kalogera. The mass distribution of stellar-mass black holes. *The Astrophysical Journal*, 741(2):103, 2011.

[15] T. Fragos, M. Tremmel, E. Rantsiou, and K. Belczynski. Black hole spin–orbit misalignment in galactic x-ray binaries. *The Astrophysical Journal Letters*, 719(1):L79, 2010.

[16] V. P. Frolov and A. Zelnikov. Introduction to black hole physics. 2011.

[17] C. S. Froning and E. L. Robinson. Near-infrared light curves of the black hole binary a0620- 00. *The Astronomical Journal*, 121(4):2212, 2001.

[18] C. S. Froning, E. L. Robinson, and M. A. Bitner. Near-infrared spectra of the black hole x-ray binary a0620-00. *The Astrophysical Journal*, 663(2):1215, 2007.

[19] D. M. Gelino, T. E. Harrison, and J. A. Orosz. A multiwavelength, multiepoch study of the soft x-ray transient prototype, v616 monocerotis (a0620- 00). *The Astronomical Journal*, 122(5):2668, 2001.

[20] L. Gou, J. E. McClintock, M. J. Reid, J. A. Orosz, J. F. Steiner, R. Narayan, J. Xiang, R. A. Remillard, K. A. Arnaud, and S. W. Davis. The extreme spin of the black hole in cygnus x-1. *The Astrophysical Journal*, 742(2):85, 2011.

[21] J. Gribbin. *Companion to the Cosmos*. Little, Brown, 1997.

[22] C. A. Haswell, E. L. Robinson, K. Horne, R. F. Stiening, and T. Abbott. On the mass of the compact object in the black hole binary a0620-00. *The Astrophysical Journal*, 411:802–812, 1993.

[23] R. Hynes, P. Charles, J. Casares, C. Haswell, C. Zurita, and T. Shahbaz. Fast photometry of quiescent soft x-ray transients with the acquisition camera on gemini-south. *Monthly Notices of the Royal Astronomical Society*, 340(2):447–456, 2003.

[24] V. Kalogera and G. Baym. The maximum mass of a neutron star. *The Astrophysical Journal Letters*, 470(1):L61, 1996.

[25] S. Kato. Mass and spin of grs 1915 105 based on a resonance model of qpos. *Publications of the Astronomical Society of Japan*, 56(5):L25–L28, 2004.

[26] S. Kato. A vertical resonance of g-mode oscillations in warped disks and qpos in low-mass x-ray binaries. *Publications of the Astronomical Society of Japan*, 57(4):699–703, 2005.

[27] K. I. Koljonen and T. J. Maccarone. Gemini/gnirs infrared spectroscopy of the wolf–rayet stellar wind in cygnus x-3. *Monthly Notices of the Royal Astronomical Society*, 472(2):2181–2195, 2017.

[28] E. D. Kovetz, I. Cholis, P. C. Breysse, and M. Kamionkowski. Black hole mass function from gravitational wave measurements. *Physical Review D*, 95(10):103010, 2017.

[29] E. M. Leibowitz, S. Hemar, and M. Orio. Regularities in the long-term optical light curve of the black hole candidate binary a0620—00 (v616 mon). *Monthly Notices of the Royal Astronomical Society*, 300(2):463–468, 1998.

[30] J. Liu, H. Zhang, A. W. Howard, Z. Bai, Y. Lu, R. Soria, S. Justham, X. Li, Z. Zheng, T. Wang, et al. A wide star–black-hole binary system from radial-velocity measurements. *Nature*, 575(7784):618–621, 2019.

[31] R. K. MacDonald, C. D. Bailyn, M. Buxton, A. G. Cantrell, R. Chatterjee, R. Kennedy-Shaffer, J. A. Orosz, C. B. Markwardt, and J. H. Swank. The black hole binary v4641 sagitarii: Activity in quiescence and improved mass determinations. *The Astrophysical Journal*, 784(1):2, 2014.

[32] J. McClintock and R. Remillard. The black hole binary a0620-00. *The Astrophysical Journal*, 308:110–122, 1986.

[33] J. E. McClintock, R. Narayan, S. W. Davis, L. Gou, A. Kulkarni, J. A. Orosz, R. F. Penna, R. A. Remillard, and J. F. Steiner. Measuring the spins of accreting black holes. *Classical and Quantum Gravity*, 28(11):114009, 2011.

[34] J. Miller, C. Reynolds, A. Fabian, G. Miniutti, and L. Gallo. Stellar-mass black hole spin constraints from disk reflection and continuum modeling. *The Astrophysical Journal*, 697(1):900, 2009.

[35] W. R. Morningstar and J. M. Miller. The spin of the black hole 4u 1543-47. *The Astrophysical Journal Letters*, 793(2):L33, 2014.

[36] S. Motta, T. Belloni, L. Stella, T. Muñoz-Darias, and R. Fender. Precise mass and spin measurements for a stellar-mass black hole through x-ray timing: The case of gro j1655- 40. *Monthly Notices of the Royal Astronomical Society*, 437(3):2554–2565, 2014.

[37] S. E. Motta. Quasi periodic oscillations in black hole binaries. *Astronomische Nachrichten*, 337(4-5):398–403, 2016.

[38] A. B. Nielsen. On the distribution of stellar-sized black hole spins. In *Journal of Physics: Conference Series*, volume 716, page 012002. IOP Publishing, 2016.

[39] D. O'Donoghue and P. Charles. Have superhumps been seen in black hole soft x-ray transients? *Monthly Notices of the Royal Astronomical Society*, 282(1):191–205, 1996.

[40] J. A. Orosz and C. D. Bailyn. Optical observations of gro j1655–40 in quiescence. i. a precise mass for the black hole primary. *The Astrophysical Journal*, 477(2):876, 1997.

[41] J. A. Orosz and P. H. Hauschildt. The use of the nextgen model atmospheres for cool giants in a light curve synthesis code. *arXiv preprint astro-ph/0010114*, 2000.

[42] J. A. Orosz, J. E. McClintock, J. P. Aufdenberg, R. A. Remillard, M. J. Reid, R. Narayan, and L. Gou. The mass of the black hole in cygnus x-1. *The Astrophysical Journal*, 742(2):84, 2011.

[43] F. Özel, D. Psaltis, R. Narayan, and J. E. McClintock. The black hole mass distribution in the galaxy. *The Astrophysical Journal*, 725(2):1918, 2010.

[44] M. J. Reid, J. E. McClintock, R. Narayan, L. Gou, R. A. Remillard, and J. A. Orosz. The trigonometric parallax of cygnus x-1. *The Astrophysical Journal*, 742(2):83, 2011.

[45] R. A. Remillard and J. E. McClintock. X-ray properties of black-hole binaries. *Annu. Rev. Astron. Astrophys.*, 44:49–92, 2006.

[46] B. Sathyaprakash, M. Abernathy, F. Acernese, P. Amaro-Seoane, N. Andersson, K. Arun, F. Barone, B. Barr, M. Barsuglia, M. Beker, et al. Scientific potential of einstein telescope. *arXiv preprint arXiv:1108.1423*, 2011.

[47] R. Shafee, J. E. McClintock, R. Narayan, S. W. Davis, L.-X. Li, and R. A. Remillard. Estimating the spin of stellar-mass black holes by spectral fitting of the x-ray continuum. *The Astrophysical Journal Letters*, 636(2):L113, 2005.

[48] T. Shahbaz, T. Naylor, and P. Charles. The mass of the black hole in. *Monthly Notices of the Royal Astronomical Society*, 268(3):756–762, 1994.

[49] H. Shibahashi and S. J. Murphy. Search for quiet stellar-mass black holes by asteroseismology from space. *arXiv preprint arXiv:1912.08396*, 2019.

[50] R. A. Wade and K. Horne. The radial velocity curve and peculiar tio distribution of the red secondary star in z chamaeleontis. *The Astrophysical Journal*, 324:411–430, 1988.

[51] A. Zakharov, F. De Paolis, G. Ingrosso, and A. Nucita. Direct measurements of black hole charge with future astrometrical missions. *Astronomy & Astrophysics*, 442(3):795–799, 2005.

[52] C. Zurita, J. Casares, and T. Shahbaz. Evidence for optical flares in quiescent soft x-ray transients. *The Astrophysical Journal*, 582(1):369, 2003.